
The Generalized Eigenvalue Problem as a Nash Equilibrium

Ian Gemp*

DeepMind

London, UK

imgemp@deepmind.com

Charlie Chen*

DeepMind

London, UK

ccharlie@deepmind.com

Brian McWilliams

DeepMind

London, UK

bmcw@deepmind.com

Abstract

The generalized eigenvalue problem (GEP) is a fundamental concept in numerical linear algebra. It captures the solution of many classical machine learning problems such as canonical correlation analysis, independent components analysis, partial least squares, linear discriminant analysis, principal components, successor features and others. Despite this, most general solvers are prohibitively expensive when dealing with massive data sets and research has instead concentrated on finding efficient solutions to specific problem instances. In this work, we develop a game-theoretic formulation of the top- k GEP whose Nash equilibrium is the set of generalized eigenvectors. We also present a parallelizable algorithm with guaranteed asymptotic convergence to the Nash. Current state-of-the-art methods require $\mathcal{O}(d^2k)$ complexity per iteration which is prohibitively expensive when the number of dimensions (d) is large. We show how to achieve $\mathcal{O}(dk)$ complexity, scaling to datasets 100× larger than those evaluated by prior methods. Empirically we demonstrate that our algorithm is able to solve a variety of GEP problem instances including a large-scale analysis of neural network activations.

1 Introduction

This work considers the generalized eigenvalue problem (GEP),

$$Av = \lambda Bv \tag{1}$$

where A is symmetric and B is symmetric, positive definite. While the GEP is not a common sight in modern machine learning literature, remarkably it actually underlies several fundamental problems. Most obviously, when $A = X^\top X$, $B = I$, and X is a data matrix, we recover the ubiquitous SVD/PCA. However, by considering other forms of the A and B matrices we recover other well known problems. These include, but are not limited to:

Canonical Correlation Analysis (CCA): Given a dataset of *paired* observations (or views) $x \in \mathbb{R}^{d_x}$ and $y \in \mathbb{R}^{d_y}$ (e.g., gene expressions x and medical imaging y corresponding to the same patient), CCA returns the linear projections of x and y that are maximally correlated. CCA is particularly useful for learning multi-modal representations of data and in semi-supervised learning [29]; it is effectively the multi-view generalization of PCA [18, 32]

*Asterisk denotes equal contribution.

where A and B contain the cross- and auto-covariances of the two views respectively:

$$A = \begin{bmatrix} \mathbf{0} & \mathbb{E}[xy^\top] \\ \mathbb{E}[yx^\top] & \mathbf{0} \end{bmatrix} \quad B = \begin{bmatrix} \mathbb{E}[xx^\top] & \mathbf{0} \\ \mathbf{0} & \mathbb{E}[yy^\top] \end{bmatrix}. \quad (2)$$

Independent Component Analysis (ICA): ICA seeks the directions in the data which are most structured, or alternatively, appear least Gaussian [20]. A common GEP formulation of ICA uncovers latent variables which maximize the non-Gaussianity of the data as defined by its excess kurtosis. ICA has famously been proposed as a solution to the so-called cocktail party source-separation problem in audio processing and has been used for denoising and more generally, the discovery of explanatory latent factors in data. Here A and B are the excess kurtosis and the covariance of the data respectively:

$$A = \mathbb{E}[\langle x, x \rangle xx^\top] - \text{tr}(B)B - 2B^2 \quad B = \mathbb{E}[xx^\top]. \quad (3)$$

Normalized Graph Laplacians: The graph Laplacian matrix (L) is central to tasks such as spectral clustering ($A = L$, $B = I$) where its eigenvectors are known to solve a relaxation of min-cut [44]. Alternatives, such as the random walk normalized Laplacian ($A = L$, B is the diagonal node-degree matrix), approximate other min-cut objectives. These normalized variants, in particular, are important to computing representations for learning value functions in reinforcement learning such as successor features [25, 39, 26], an extension of proto-value functions [27] which uses the un-normalized graph Laplacian ($A = L$, $B = I$).

Partial least squares (PLS) can be formulated similarly to CCA and finds extensive use in chemometrics [8] and medical domains [3]. Likewise, linear discriminant analysis (LDA) can be formulated as a GEP and learns a label-aware projection of the data that separates classes well [11, 36]. More examples and uses of the GEP can be found in [6, 7]. We now shift focus to the mathematical properties and challenges of the corresponding GEP.

The matrices A and B above can either be defined using expectations under a data distribution (e.g., $\mathbb{E}_{x \sim p(x)}[xx^\top]$) or means over a finite sample dataset (e.g., $\frac{1}{n}X^\top X$ where $X \in \mathbb{R}^{n \times d_x}$). In either case, we typically assume the data has mean zero unless specified otherwise.

Note that the GEP, $Av = \lambda Bv$, is *similar* to the eigenvalue problem, $B^{-1}Aw = \lambda'w$, in a formal sense (see Proposition 3 in Appx. A). There are two reasons for working with the GEP instead: 1) inverting B is prohibitively expensive for a large matrix and 2) while A and $B \succ 0$ are symmetric, $B^{-1}A$ is not, which hides useful information about the eigenvalues and eigenvectors (they are necessarily real and B -orthogonal). This also highlights that the GEP is a fundamentally more challenging problem than SVD and why a direct application of previous game-theoretic approaches such as [15, 16] is not possible.

The complexity of solving the GEP is $\mathcal{O}(d^3)$ where d is the dimension of the square matrix A (equiv. B). Several libraries exist for solving the GEP in-memory [42]. For example, `scipy` calls LAPACK which solves the GEP via a Schur decomposition.

The in-memory implementations of GEP solvers are quite sophisticated. In contrast, machine learning research has developed simple approximate solvers for singular value decomposition (SVD) that scale to very large datasets [2]. It is surprising, given the importance of the GEP to machine learning and statistics, that we do not yet have a simple, iterative solution to this problem. In this work, we contribute the first simple, elegant solution to this root problem of machine learning and statistics, including

- A game whose Nash equilibrium is the top- k GEP solution,
- An easily parallelizable algorithm with $\mathcal{O}(dk)$ per-iteration complexity relying only on matrix-vector products,
- An empirical evaluation on problems 100 \times larger than previous state-of-the-art.

The game and accompanying algorithm are developed synergistically to achieve a formulation that is amenable to analysis and naturally leads to an elegant and efficient algorithm.

2 Generalized EigenGame: Players, Strategies, and Utilities

In this work, we take the approach of defining the GEP as a game. It is an open question how to define a game appropriately such that key properties of the GEP are captured. As argued in previous work [15, 16], game formulations make obvious how computation can be distributed over players, leading to high parallelization, which is critical for processing large datasets. They have also clarified geometrical properties of the problem.

Specifically, we are interested in solving the top- k GEP which means we are interested in finding the (unit-norm) generalized eigenvectors \hat{v}_i associated with the top- k largest generalized eigenvalues λ_i . Therefore, let there be k **players** denoted $i \in \{1, \dots, k\}$, and let each select a vector \hat{v}_i (**strategy**) from the unit-sphere \mathcal{S}^{d-1} (*strategy space*). We define player i 's **utility** function conditioned on its parents (players $j < i$) as follows:

$$u_i(\hat{v}_i | \hat{v}_{j < i}) = \overbrace{\frac{\langle \hat{v}_i, A\hat{v}_i \rangle}{\langle \hat{v}_i, B\hat{v}_i \rangle}}^{\text{generalized Rayleigh Quotient}} - \sum_{j < i} \frac{\langle \hat{v}_j, A\hat{v}_j \rangle \langle \hat{v}_i, B\hat{v}_j \rangle^2}{\langle \hat{v}_j, B\hat{v}_j \rangle^2 \langle \hat{v}_i, B\hat{v}_i \rangle} \quad (4)$$

$$= \underbrace{\hat{\lambda}_i}_{\text{reward}} - \sum_{j < i} \underbrace{\hat{\lambda}_j \langle \hat{y}_i, B\hat{y}_j \rangle^2}_{\text{penalty}} \quad \text{where } \hat{y}_i = \frac{\hat{v}_i}{\|\hat{v}_i\|_B}, \quad (5)$$

$$\hat{\lambda}_i = \frac{\langle \hat{v}_i, A\hat{v}_i \rangle}{\langle \hat{v}_i, B\hat{v}_i \rangle}, \text{ and } \|z\|_B = \sqrt{\langle z, Bz \rangle}.$$

Player i 's utility has an intuitive explanation. The first term is recognized as the generalized Rayleigh quotient which can be derived by left multiplying both sides of the GEP ($v^\top Av = \lambda v^\top Bv$) and solving for λ . Note that the generalized eigenvectors are guaranteed to be B -orthogonal, i.e., $v_i^\top Bv_j = 0$ for all $i \neq j$ (see Lemma 2 in Appx. A). Therefore, the **reward** term incentivizes players to find directions that result in large eigenvalues, but are simultaneously **penalized** for choosing directions that align with directions chosen by their parents (players with index less than i , higher in the hierarchy). Finally, the penalty coefficient $\hat{\lambda}_j$ serves to balance the magnitude of the penalty terms with the reward term such that players have no incentive to “overlap” with parents. We formally prove that these utilities are well-posed in the sense that, given exact parents, their optima coincide with the top- k GEP solution.

Lemma 1 (Well-posed Utilities). *Given exact parents and assuming the top- k eigenvalues of $B^{-1}A$ are distinct and positive, the maximizer of player i 's utility is the unique generalized eigenvector v_i (up to sign, i.e., $-v_i$ is also valid).*

Note that $\hat{\lambda}_i = \frac{\langle \hat{v}_i, A\hat{v}_i \rangle}{\langle \hat{v}_i, B\hat{v}_i \rangle} = \frac{\langle \hat{v}_i / \|\hat{v}_i\|_B, A\hat{v}_i / \|\hat{v}_i\|_B \rangle}{\langle \hat{v}_i / \|\hat{v}_i\|_B, B\hat{v}_i / \|\hat{v}_i\|_B \rangle} = \frac{\langle \hat{y}_i, A\hat{y}_i \rangle}{\langle \hat{y}_i, B\hat{y}_i \rangle}$, therefore, the above results still hold for utilities defined using vectors constrained to the unit ellipsoid, $\|\hat{y}_i\|_B = 1$, rather than the unit-sphere, $\|\hat{v}_i\|_I = 1$. However, in cases we are interested in, B is a massive matrix which can never be explicitly constructed and instead only observed via minibatches. It is then not clear how to handle the constraint $\|\hat{y}_i\|_B = 1$. We therefore only consider an approach that constrains the solution to the unit sphere $\|\hat{v}_i\|_I = 1$.

Next, we provide intuition for the shape of these utilities. Surprisingly, while non-concave, we prove analytically in Appx. B that they have a simple sinusoidal shape. A numerical illustration is given in Figure 1 to help the reader visualize this property.

Proposition 1 (Utility Shape). *Each player's utility is periodic in the angular deviation (θ) along the sphere. Its shape is sinusoidal, but with its angular axis (θ) smoothly deformed as a function of B . Most importantly, every local maximum is a global maximum.*

Figure 1 illustrates a primary difficulty of solving the GEP over SVD. Due to the extreme differences in curvature caused by the B matrix, the GEP should benefit from optimizers employing adaptive per-dimension learning rates. To our knowledge, this characterization of the difficulty of the GEP is novel and we exploit this insight in experiments.

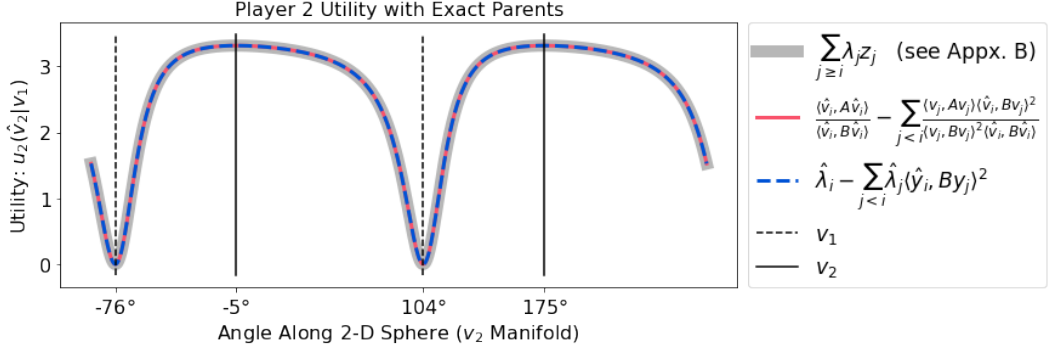


Figure 1: Each player’s utility is a sinusoid on the sphere warped tangentially along the axis of angular deviation according to B ; values for A and B used in this example are given in Appx. B. Three mathematical representations of the utility are plotted; their equivalence is supported by the overlapping curves. If player 2 aligns with the top eigenvector (dashed vertical), they receive zero utility. If they align with the second eigenvector (solid vertical), they receive the second eigenvalue (optimal) as reward. If $B = I$ as in SVD/PCA, the vertical lines indicating the minima and maxima would be separated by exactly 90° . In this case, the matrix B redefines what it means for two vectors to be orthogonal ($\langle \hat{v}_i, B\hat{v}_j \rangle = 0$), so that the vectors are 71° (equivalently, $180^\circ - 71^\circ = 109^\circ$) from each other.

Finally, we formally define our proposed game and prove its equilibrium constitutes the top- k GEP solution. We use the Greek letter *gamma* to denote *generalized*, and we differentiate between the game and the algorithm with upper Γ and lower case γ respectively.

Definition 1 (Γ -EigenGame). *Let Γ -EigenGame be the game with players $i \in \{1, \dots, k\}$, their strategy spaces $\hat{v}_i \in \mathcal{S}^{d-1}$, and their utilities u_i as defined in equation (5).*

Theorem 1 (Nash Property). *Assuming the top- k generalized eigenvalues of the generalized eigenvalue problem $Av = \lambda Bv$ are positive and distinct, their corresponding generalized eigenvectors form the unique, strict Nash equilibrium of Γ -EigenGame.*

Proof. Lemma 1 proves that each generalized eigenvector v_i ($i \in \{1, \dots, k\}$) is the unique best response to v_{-i} , which implies the entire set constitutes the unique Nash equilibrium. \square

3 Algorithm: Unbiased Player Updates and Auxiliary Variables

Given that Γ -EigenGame suitably captures the top- k GEP, we now develop an iterative algorithm to approximate its solution. The basic approach we take is to perform parallel gradient ascent on all player utilities simultaneously. We will first write down the gradient of each player’s utility and then introduce several simplifications for the purpose of enabling unbiased estimates in the stochastic setting.

Up to scaling factors, the gradient of player i ’s utility function with respect to \hat{v}_i is

$$\frac{(\hat{v}_i^\top B\hat{v}_i)A\hat{v}_i - (\hat{v}_i^\top A\hat{v}_i)B\hat{v}_i}{\langle \hat{v}_i, B\hat{v}_i \rangle^2} - \sum_{j < i} \frac{\hat{\lambda}_j}{\langle \hat{v}_j, B\hat{v}_j \rangle} \frac{(\hat{v}_i^\top B\hat{v}_j) - \langle \hat{v}_i, B\hat{v}_j \rangle B\hat{v}_i}{\langle \hat{v}_i, B\hat{v}_i \rangle^2}. \quad (6)$$

Recall that B is a matrix that we intend to estimate with samples, i.e., it is a random variable, and it appears several times in the denominator of the gradient. Obtaining unbiased estimates of inverses of random variables is difficult (e.g., the naive approach gives an overestimate; $\mathbb{E}[1/x] \geq 1/\mathbb{E}[x]$ by Jensen’s inequality). We can remove the scalar $\langle \hat{v}_i, B\hat{v}_i \rangle^2$ in the denominator because it is common to all terms and will not change the direction of the gradient nor the location of fixed points; this step is critical to the design of our stochastic algorithm which we will explain later. We also use the following two additional relations:

- (i) $\hat{\lambda}_j \langle \hat{v}_i, B\hat{v}_j \rangle = \langle \hat{v}_i, A\hat{v}_j \rangle$ if player i ’s parents match their true solutions, i.e., $\hat{v}_{j < i} = v_{j < i}$,

$$(ii) \langle \hat{v}_j, B\hat{v}_j \rangle = \sqrt{\langle \hat{v}_j, B\hat{v}_j \rangle^2} = \|\hat{v}_j\|_B^2 \text{ because } B \succ 0,$$

to arrive at the simplified update direction

$$\tilde{\nabla}_i = \underbrace{(\hat{v}_i^\top B\hat{v}_i)A\hat{v}_i - (\hat{v}_i^\top A\hat{v}_i)B\hat{v}_i}_{\text{reward}} - \sum_{j < i} \underbrace{(\hat{v}_i^\top A\hat{y}_j)[\langle \hat{v}_i, B\hat{v}_i \rangle B\hat{y}_j - \langle \hat{v}_i, B\hat{y}_j \rangle B\hat{v}_i]}_{\text{penalty}}. \quad (7)$$

Simplifying the gradient using (i) is sound because the hierarchy of players ensures the parents will be learned exactly asymptotically. For instance, player 1's update has no penalty terms and so will converge asymptotically. The argument then proceeds by induction.

Note that B still appears in the denominator via the \hat{y}_j terms (recall equation (5)). We will revisit this issue later, but for now we will show this update converges to the desired solution given exact estimates of expectations (full-batch setting).

Proposition 2. *The direction $\tilde{\nabla}_i$ defined in equation (7) is a steepest ascent direction on utility $u_i(\hat{v}_i | \hat{v}_{j < i})$ given exact parents $\hat{v}_{j < i} = v_{j < i}$.*

Proof. This fact follows from the above argument that removing a positive scalar multiplier does not change the direction of the gradient of u_i w.r.t. \hat{v}_i and applying relation (i). \square

We present the deterministic version of γ -EigenGame in Algorithm 1 where k players use $\tilde{\nabla}_i$ in (7) to maximize their utilities in parallel (see **parfor**-loop below). While simultaneous gradient ascent fails to converge to Nash equilibria in games in general, it succeeds in this case because the hierarchy we impose ensures each player has a unique best response (Lemma 1); this type of procedure is known as *iterative strict dominance* in the game theory literature. Theorem 2, proven in Appx. E, guarantees it converges asymptotically to the true solution.

Algorithm 1 Deterministic / Full-batch γ -EigenGame

```

1: Given:  $A \in \mathbb{R}^{d \times d}$  and  $B \in \mathbb{R}^{d \times d}$ , step size sequence  $\eta_t$ , and number of iterations  $T$ .
2:  $\hat{v}_i \sim \mathcal{S}^{d-1}$ , i.e.,  $\hat{v}_i \sim \mathcal{N}(\mathbf{0}_d, \mathbf{I}_d)$ ;  $\hat{v}_i \leftarrow \hat{v}_i / \|\hat{v}_i\|$  for all  $i$ 
3: for  $t = 1 : T$  do
4:   parfor  $i = 1 : k$  do
5:      $\hat{y}_j = \frac{\hat{v}_j}{\sqrt{\langle \hat{v}_j, B\hat{v}_j \rangle}}$ 
6:     rewards  $\leftarrow (\hat{v}_i^\top B\hat{v}_i)A\hat{v}_i - (\hat{v}_i^\top A\hat{v}_i)B\hat{v}_i$ 
7:     penalties  $\leftarrow \sum_{j < i} (\hat{v}_i^\top A\hat{y}_j)[\langle \hat{v}_i, B\hat{v}_i \rangle B\hat{y}_j - \langle \hat{v}_i, B\hat{y}_j \rangle B\hat{v}_i]$ 
8:      $\tilde{\nabla}_i \leftarrow \text{rewards} - \text{penalties}$ 
9:      $\hat{v}'_i \leftarrow \hat{v}_i + \eta_t \tilde{\nabla}_i$ 
10:     $\hat{v}_i \leftarrow \frac{\hat{v}'_i}{\|\hat{v}'_i\|}$ 
11:  end parfor
12: end for
13: return all  $\hat{v}_i$ 

```

Theorem 2 (Deterministic / Full-batch Global Convergence). *Given a symmetric matrix A and symmetric positive definite matrix B where the top- k eigengaps of $B^{-1}A$ are positive along with a square-summable, not summable step size sequence η_t (e.g., $1/t$), Algorithm 1 converges to the top- k generalized eigenvectors asymptotically ($\lim_{T \rightarrow \infty}$) with probability 1.*

In the big data setting, A and B are statistical estimates, i.e., expectations of quantities over large datasets. Precomputing exact estimates is computationally expensive, so we assume a data model that allows drawing small *minibatches* of data at a time. Under such a model, stochastic approximation theory typically guarantees that as long as the update directions are *unbiased*, i.e., equal in expectation to the updates with exact estimates, then an appropriate algorithm will converge to the true solution.

Algorithm 2 Stochastic γ -EigenGame

```

1: Given: paired data streams  $X_t \in \mathbb{R}^{b \times d_x}$  and  $Y_t \in \mathbb{R}^{b \times d_y}$ , number of parallel machines  $M$  per player (minibatch size per machine  $b' = \frac{b}{M}$ ), step size sequences  $\eta_t$  and  $\gamma_t$ , scalar  $\rho$  lower bounding  $\sigma_{\min}(B)$ , and number of iterations  $T$ .
2:  $\hat{v}_i \sim \mathcal{S}^{d-1}$ , i.e.,  $\hat{v}_i \sim \mathcal{N}(\mathbf{0}_d, \mathbf{I}_d)$ ;  $\hat{v}_i \leftarrow \hat{v}_i / \|\hat{v}_i\|$  for all  $i$ 
3:  $[B\hat{v}]_i \leftarrow \hat{v}_i^0$  for all  $i$ 
4: for  $t = 1 : T$  do
5:   parfor  $i = 1 : k$  do
6:     parfor  $m = 1 : M$  do
7:       Construct  $A_{tm}$  and  $B_{tm}$  (*unbiased estimates using independent data batches)
8:        $\hat{y}_j = \frac{\hat{v}_j}{\sqrt{\max(\langle \hat{v}_j, [B\hat{v}]_j \rangle, \rho)}}$ 
9:        $[B\hat{y}]_j = \frac{[B\hat{v}]_j}{\sqrt{\langle \hat{v}_j, [B\hat{v}]_j \rangle \rho}}$ 
10:      rewards  $\leftarrow (\hat{v}_i^\top B_{tm} \hat{v}_i) A_{tm} \hat{v}_i - (\hat{v}_i^\top A_{tm} \hat{v}_i) B_{tm} \hat{v}_i$ 
11:      penalties  $\leftarrow \sum_{j < i} (\hat{v}_i^\top A \hat{y}_j) [\langle \hat{v}_i, B_{tm} \hat{v}_i \rangle [B\hat{y}]_j - \langle \hat{v}_i, [B\hat{y}]_j \rangle B_{tm} \hat{v}_i]$ 
12:       $\tilde{\nabla}_{im} \leftarrow \text{rewards} - \text{penalties}$ 
13:       $\nabla_{im}^{Bv} = (B_{tm} \hat{v}_i - [B\hat{v}]_i)$ 
14:    end parfor
15:     $\tilde{\nabla}_i \leftarrow \frac{1}{M} \sum_m [\tilde{\nabla}_{im}]$ 
16:     $\hat{v}'_i \leftarrow \hat{v}_i + \eta_t \tilde{\nabla}_i$ 
17:     $\hat{v}_i \leftarrow \frac{\hat{v}'_i}{\|\hat{v}'_i\|}$ 
18:     $\nabla_i^{Bv} \leftarrow \frac{1}{M} \sum_m [\nabla_{im}^{Bv}]$ 
19:     $[B\hat{v}]_i \leftarrow [B\hat{v}]_i + \gamma_t \nabla_i^{Bv}$ 
20:  end parfor
21: end for
22: return all  $\hat{v}_i$ 

```

In order to construct an unbiased update direction given access to minibatches of data, we need to draw multiple minibatches independently at random. We can construct an unbiased estimate of products of expectations, e.g., $(\hat{v}_i^\top B \hat{v}_i) A \hat{v}_i$, by drawing an independent batch for each, e.g., one for B and one for A . However, the B that appears in the denominator of \hat{y}_j is problematic; we cannot construct an unbiased estimate of the inverse of a random variable.

These problematic \hat{y}_j terms only appear in the penalties, which are a function of the parents' eigenvector approximations. The first eigenvector has no parents, and so we can easily construct an unbiased estimate for it using multiple minibatches. We can then construct an unbiased estimate for each subsequent player by inductive reasoning. Intuitively, once the parents have been learned, \hat{v}_j should be stable and so it should be possible to estimate $B\hat{v}_j$ from a running average, and in turn, \hat{y}_j . This suggests introducing an auxiliary variable, denoted $[B\hat{v}]_j$ to track the running averages of $B\hat{v}_j$ (a similar approach is employed in [34]). This effectively replaces $B\hat{y}_j$ with a non-random variable, avoiding the bias dilemma, at the expense of doubling the number of variables. Note that introducing this auxiliary variable implies the inner product $\langle \hat{v}_j, [B\hat{v}]_j \rangle$ may not be positive definite, therefore, we manually clip the result to be greater than or equal to ρ , the minimum singular value of B .

Precise pseudocode for this approach is given in Algorithm 2. Differences to Algorithm 1 are highlighted in color (auxiliary differences in blue, clipping in red). We point out that introducing an auxiliary variable for player i to track $[B\hat{v}]_i$ is not feasible because unlike player i 's parents' variables, \hat{v}_i cannot be assumed to be non-stationary. This is why removing $\langle \hat{v}_i, B\hat{v}_i \rangle^2$ earlier from the denominator of equation (6) was critical. Lastly, note that these modifications to the update are derived using an understanding of the intended computation and theoretical considerations; put shortly, *autograd* libraries will not uncover this solution. See Appx. E.2 for more discussion and analysis of Algorithm 2.

Computational Complexity and Parallelization. The naive, per-iteration cost of this update is $\mathcal{O}(bdk^2)$ with batch size b , but we can easily achieve both model and data

parallelism to reduce this. If each player (model) parallelizes over $M = b$ machines (data) as indicated by the two **parfor**-loops, the complexity reduces to $\mathcal{O}(dk)$. This is easy to implement with modern libraries, e.g., `pmap` using Jax. Alternative parallel implementations are discussed in Appx. F. Lastly, the update consists purely of inexpensive elementwise operations and matrix-vector products that can be computed quickly on deep learning hardware (e.g., GPUs and TPUs); unlike previous state-of-the-art, no calls to CPU-bound linear algebra subroutines are necessary.

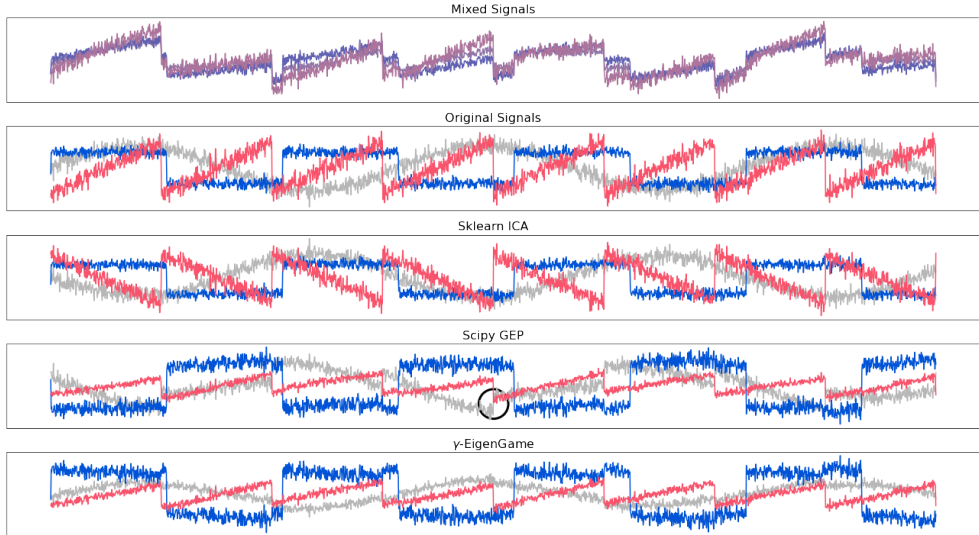


Figure 2: Blind Source Separation. Algorithm 2 (γ -EigenGame) run for 1000 epochs with minibatches of size $\frac{n}{4}$ subsampled i.i.d. from the dataset recovers the three original signals from the linearly mixed signals. Scikit-learn’s FastICA² also recovers the signals by maximizing an alternative measure of non-Gaussianity. Directly solving the GEP using `scipy.linalg.eigh(A, B)` fails to cleanly recover the gray sinusoid (black circle highlights a discontinuity) due to overfitting to the sample dataset. We confirm this by training γ -EigenGame for many more iterations and show it exhibits similar artifacts in Appx. G.

4 Related Work

The GEP is a fundamental problem in numerical linear algebra with numerous applications in machine learning and statistics. To our knowledge the most efficient approaches for the GEP or specific GEP sub-problems (e.g., CCA) scale at best $\mathcal{O}(d^2k)$ in the streaming setting. None of the current top- k solvers are simple. We summarize some of these approaches here.

Ge et al. [13] give an algorithm for top- k GEP that makes repeated use of a linear system solver to approximate the subspace of the true generalized eigenvectors, but may return an arbitrary rotation of the solution. While their method is theoretically efficient, it requires precomputing A and B which prohibits its use in a streaming data setting. The sequential least squares CCA algorithm proposed by [45] similarly requires access to the full dataset up front, however, in their case, it is to ensure the generalized eigenvectors are exactly unit-norm relative to the matrix B . Allen-Zhu and Li [1] develop a GEP algorithm that is theoretically linear in the size of the input (nd) and k , however, they assume access to the entire dataset (non-streaming). Arora et al. [4] propose a convex relaxation of the CCA problem along with a streaming algorithm with convergence guarantees. However, instead of learning $V_x \in \mathbb{R}^{d_x}$ and $V_y \in \mathbb{R}^{d_y}$ directly, it learns $M = V_x V_y^\top \in \mathbb{R}^{d_x \times d_y}$ which is prohibitively expensive to store in memory for high-dimensional problems. Moreover, the complexity of this algorithm is $\mathcal{O}(d^3)$ due to an expensive projection step requiring an SVD of M . They propose an alternative version *without* guarantees that reduces the cost per iteration to $\mathcal{O}(dk^2)$. Gao

²Run with `logcosh` approximation to negentropy (see [20] for explanation).

et al. [12] also considers the streaming setting, but instead focuses on top-1 CCA and like [45] and [1], uses shift-invert preconditioning to accelerate convergence. Bhatia et al. [5] solves top-1 GEP in the streaming setting, only solving for the principal generalized eigenvector. Most recently, Meng et al. [30] proposed a method to estimate top- k CCA in a streaming setting. Their algorithm requires several expensive Riemannian optimization subroutines, giving a per iteration complexity of $\mathcal{O}(d^2k)$. Their convergence guarantee is in terms of subspace error, so as mentioned above, the projection matrices V_x and V_y may be rotations of their ordered (by correlation) counterparts. Their approach is the current state-of-the-art when considering CCA in the streaming setting for large datasets.

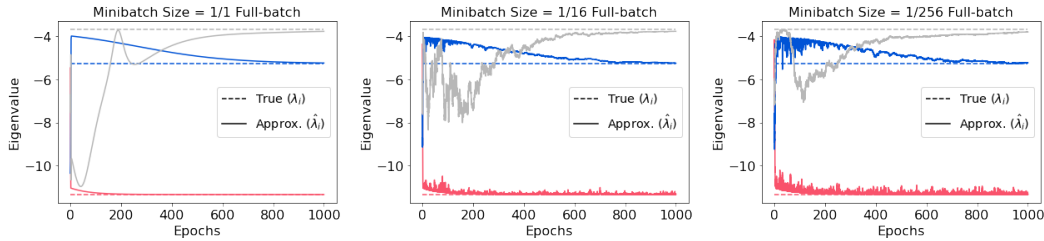


Figure 3: γ -EigenGame converges to the true GEP solution regardless of minibatch size in support of the unbiased nature of the derived update scheme (Algorithm 2).

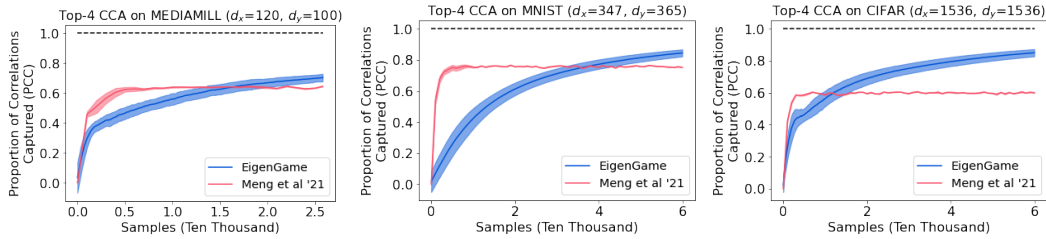


Figure 4: γ -EigenGame compared against [30]. Optimal performance denoted by dashed line. Proportion of correlations captured is $\sum_i^k \hat{\lambda}_i / \sum_i^k \lambda_i$. Shading indicates ± 1 stdev.

5 Experiments

We demonstrate our proposed stochastic approach, Algorithm 2, on solving ICA and CCA via their GEP formulations, and provide empirical support for its veracity. We plan to open source this approach in Jax. Scipy’s `linalg.eigh(A, B)`[43] is treated as ground truth when the data size permits. Hyperparameters are listed in Appx. H.

5.1 ICA

As mentioned in the introduction, ICA can be used to disentangle mixed signals such as in the cocktail party problem. Here, we use the GEP formulation to unmix three linearly mixed signals. Note that because the GEP learns a linear unmixing of the data, the magnitude (and sign) of the original signals cannot be learned. Any change in the magnitude of a signal extracted by the GEP can be offset by adjusting the magnitude and sign of a mixing weight.

We replicate a synthetic experiment from `scikit-learn`[33] and compare Algorithm 2 to several approaches. Figure 2 shows our stochastic approach (γ -EigenGame) is able to recover the shapes of the original signals (length $n = 2000$ time series).

Implicit Regularization via Fixed Step Size Updates. Note that if we run Algorithm 2 for $100\times$ more iterations with $1/10$ th the step size, we converge to the exact GEP solution (as found by `scipy`) and see similar artifacts in the extracted signals due to overfitting. Recently, Durmus et al. [10] proved that fixed step size Riemannian approximation

schemes converge to a stationary distribution around their solutions, which suggests γ -EigenGame enjoys a natural regularization property and explains its high performance on this the unmixing task. In Appx. G, we show that it is difficult to achieve similar results with `scipy` by regularizing A or B directly (e.g., $A + \epsilon I$) prior to calling `scipy.linalg.eigh`.

Unbiased Updates. Here, we empirically support our claim that the fixed point of Algorithm 2 is unbiased regardless of minibatch size.³ Not only does γ -EigenGame recover the same generalized eigenvalues, but the plots also suggests that the algorithm takes a similar trajectory for each minibatch size.

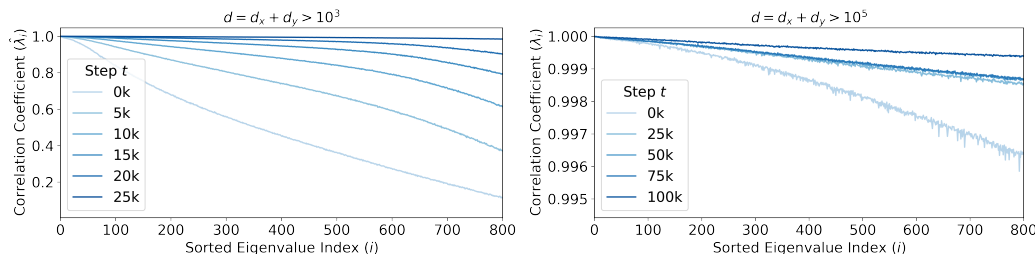


Figure 5: γ -EigenGame compares the representation (activations) of a deep network trained on CIFAR-10 for t steps to that of its final learned representation (25k or 100k steps). Curves with higher correlation coefficients indicate more similar representations.

5.2 CCA

Here, we use γ -EigenGame to linearly project multimodal datasets into lower-dimensional spaces such that they are maximally correlated.

As discussed in related work, several approaches have been developed to extend CCA to streaming, high-dimensional datasets. Recall that our approach has per-iteration complexity $\mathcal{O}(bdk)$ with the previous state-of-the-art having $\mathcal{O}(d^2k)$ [30]. We replicate the experiments of [30] and compare against their approach on three datasets.

Figure 4 shows our approach is competitive with [30]. We also point out that while their approach enjoys theoretical convergence guarantees with rates, it appears to slow in progress near a biased solution.

5.2.1 Large-scale Neural Network Analysis

Recently, CCA has been used to aid in interpreting the representations of deep neural networks [35, 31, 22]. These approaches are restricted to layer-wise comparisons of representations, reduced-dimensionality views of representations (via PCA), or small dataset sizes to accommodate current limits of CCA approaches. We replicate one of their analyses (specifically Fig. 1a of [31]) on the activations of an entire network (not just a layer), unblocking this type of analysis for larger deep learning models.

The largest dimensions handled in [35, 30] are $\mathcal{O}(10^3)$.⁴ Figure 5 demonstrates our approach (parallelized over 8 TPU chips) on $\mathcal{O}(10^3)$ dimensions (left) and $\mathcal{O}(10^5)$ dimensions (right). As mentioned in Section 2, our understanding of the geometry of the utilities suggests replacing the standard gradient ascent on \hat{v}_i with Adam [21]; Adam exhibits behavior that implicitly improves stability around equilibria [14]. For the smaller $\mathcal{O}(10^3)$ setting, where we can exactly compute ground truth using `scipy`, we confirm that our approach converges to the top-1024 (out of 2048 possible) eigenvectors with a subspace error of 0.002 (see Appx. A for computing subspace error).

³The gray line converges last because we chose to minimize rather than maximize kurtosis.

⁴Indeed, Meng et al. [30] conjecture that their approach is limited to $\mathcal{O}(10^5)$ dimensions but never demonstrate this empirically.

6 Conclusion

We presented Γ -EigenGame, a game-theoretic formulation of the generalized eigenvalue problem (GEP). Our formulation enabled the development of a novel algorithm that scales to massive datasets. The GEP underlies many classical data processing tools across the sciences, and we believe our proposed approach finally unblocks its use on the ever-growing size of modern datasets. In particular, it achieves this by parallelizing computation using modern AI-centric distributed compute infrastructure such as GPUs and TPUs.

In future work, we aim to explore improved Riemannian optimizers, analyze the theoretical convergence rate, and study alternative parallel implementations. We also plan to explore embedding our solver as a differentiable module within other machine learning pipelines.

Acknowledgements

We thank Claire Vernade for reviewing the paper and early discussions, Thore Graepel, also, for early discussions, Zhe Wang for guidance on engineering, and Sukhdeep Singh for project management.

References

- [1] Z. Allen-Zhu and Y. Li. Doubly accelerated methods for faster cca and generalized eigendecomposition. In *International Conference on Machine Learning*, pages 98–106. PMLR, 2017.
- [2] Z. Allen-Zhu and Y. Li. First efficient convergence for streaming k-PCA: a global, gap-free, and near-optimal rate. In *2017 IEEE 58th Annual Symposium on Foundations of Computer Science (FOCS)*, pages 487–492. IEEE, 2017.
- [3] A. Altmann, N. Jahanshad, P. M. Thompson, and M. Lorenzi. Partial least squares provides a whole-genome whole-brain imaging genetics approach. 2021.
- [4] R. Arora, T. V. Marinov, P. Mianjy, and N. Srebro. Stochastic approximation for canonical correlation analysis. *Advances in Neural Information Processing Systems*, 30, 2017.
- [5] K. Bhatia, A. Pacchiano, N. Flammarion, P. L. Bartlett, and M. I. Jordan. Gen-oja: Simple & efficient algorithm for streaming generalized eigenvector computation. *Advances in neural information processing systems*, 31, 2018.
- [6] T. D. Bie, N. Cristianini, and R. Rosipal. Eigenproblems in pattern recognition. In *Handbook of geometric computing*, pages 129–167. Springer, 2005.
- [7] M. Borga, T. Landelius, and H. Knutsson. *A unified approach to PCA, PLS, MLR and CCA*. Linköping University, Department of Electrical Engineering, 1997.
- [8] T. F. Boucher, M. V. Ozanne, M. L. Carmosino, M. D. Dyar, S. Mahadevan, E. A. Breves, K. H. Lepore, and S. M. Clegg. A study of machine learning regression methods for major elemental analysis of rocks using laser-induced breakdown spectroscopy. *Spectrochimica Acta Part B: Atomic Spectroscopy*, 107:1–10, 2015.
- [9] L. Deng. The mnist database of handwritten digit images for machine learning research. *IEEE Signal Processing Magazine*, 29(6):141–142, 2012.
- [10] A. Durmus, P. Jiménez, É. Moulines, and S. Salem. On riemannian stochastic approximation schemes with fixed step-size. In *International Conference on Artificial Intelligence and Statistics*, pages 1018–1026. PMLR, 2021.
- [11] R. A. Fisher. The use of multiple measurements in taxonomic problems. *Annals of eugenics*, 7(2):179–188, 1936.

- [12] C. Gao, D. Garber, N. Srebro, J. Wang, and W. Wang. Stochastic canonical correlation analysis. *J. Mach. Learn. Res.*, 20:167–1, 2019.
- [13] R. Ge, C. Jin, P. Netrapalli, A. Sidford, et al. Efficient algorithms for large-scale generalized eigenvector computation and canonical correlation analysis. In *International Conference on Machine Learning*, pages 2741–2750. PMLR, 2016.
- [14] I. Gemp and B. McWilliams. The unreasonable effectiveness of adam on cycles. In *NeurIPS Workshop on Bridging Game Theory and Deep Learning*, 2019.
- [15] I. Gemp, B. McWilliams, C. Vernade, and T. Graepel. Eigengame: PCA as a Nash equilibrium. In *International Conference for Learning Representations*, 2021.
- [16] I. Gemp, B. McWilliams, C. Vernade, and T. Graepel. Eigengame unloaded: When playing games is better than optimizing. *International Conference for Learning Representations*, 2022.
- [17] N. Goyal and A. Shetty. Sampling and optimization on convex sets in riemannian manifolds of non-negative curvature. In *Conference on Learning Theory*, pages 1519–1561. PMLR, 2019.
- [18] C. Guo and D. Wu. Canonical correlation analysis (CCA) based multi-view learning: An overview. *arXiv preprint arXiv:1907.01693*, 2019.
- [19] C. R. Harris, K. J. Millman, S. J. van der Walt, R. Gommers, P. Virtanen, D. Cournapeau, E. Wieser, J. Taylor, S. Berg, N. J. Smith, R. Kern, M. Picus, S. Hoyer, M. H. van Kerkwijk, M. Brett, A. Haldane, J. F. del Río, M. Wiebe, P. Peterson, P. Gérard-Marchant, K. Sheppard, T. Reddy, W. Weckesser, H. Abbasi, C. Gohlke, and T. E. Oliphant. Array programming with NumPy. *Nature*, 585(7825):357–362, Sept. 2020. doi: 10.1038/s41586-020-2649-2. URL <https://doi.org/10.1038/s41586-020-2649-2>.
- [20] A. Hyvärinen and E. Oja. Independent component analysis: algorithms and applications. *Neural networks*, 13(4-5):411–430, 2000.
- [21] D. P. Kingma and J. Ba. Adam: A method for stochastic optimization. *arXiv preprint arXiv:1412.6980*, 2014.
- [22] S. Kornblith, M. Norouzi, H. Lee, and G. Hinton. Similarity of neural network representations revisited. In *International Conference on Machine Learning*, pages 3519–3529. PMLR, 2019.
- [23] A. Krizhevsky, G. Hinton, et al. Learning multiple layers of features from tiny images. 2009.
- [24] Y. Liu, F. Shang, J. Cheng, H. Cheng, and L. Jiao. Accelerated first-order methods for geodesically convex optimization on Riemannian manifolds. In *Advances in Neural Information Processing Systems*, pages 4868–4877, 2017.
- [25] M. C. Machado, M. G. Bellemare, and M. Bowling. A laplacian framework for option discovery in reinforcement learning. In *International Conference on Machine Learning*, pages 2295–2304. PMLR, 2017.
- [26] M. C. Machado, C. Rosenbaum, X. Guo, M. Liu, G. Tesauro, and M. Campbell. Eigenoption discovery through the deep successor representation. *arXiv preprint arXiv:1710.11089*, 2017.
- [27] S. Mahadevan. Proto-value functions: developmental reinforcement learning. In *Proceedings of the International Conference on Machine learning*, pages 553–560, 2005.
- [28] MATLAB. 9.7.0.1190202 (R2019b). The MathWorks Inc., Natick, Massachusetts, 2018.
- [29] B. McWilliams, D. Balduzzi, and J. M. Buhmann. Correlated random features for fast semi-supervised learning. In *Advances in Neural Information Processing Systems*, pages 440–448, 2013.

[30] Z. Meng, R. Chakraborty, and V. Singh. An online riemannian pca for stochastic canonical correlation analysis. *Advances in Neural Information Processing Systems*, 34, 2021.

[31] A. Moccos, M. Raghu, and S. Bengio. Insights on representational similarity in neural networks with canonical correlation. *Advances in Neural Information Processing Systems*, 31, 2018.

[32] L. Parra and P. Sajda. Blind source separation via generalized eigenvalue decomposition. *The Journal of Machine Learning Research*, 4:1261–1269, 2003.

[33] F. Pedregosa, G. Varoquaux, A. Gramfort, V. Michel, B. Thirion, O. Grisel, M. Blondel, P. Prettenhofer, R. Weiss, V. Dubourg, J. Vanderplas, A. Passos, D. Cournapeau, M. Brucher, M. Perrot, and E. Duchesnay. Scikit-learn: Machine learning in Python. *Journal of Machine Learning Research*, 12:2825–2830, 2011.

[34] D. Pfau, S. Petersen, A. Agarwal, D. G. Barrett, and K. L. Stachenfeld. Spectral inference networks: Unifying deep and spectral learning. In *International Conference on Learning Representations*, 2018.

[35] M. Raghu, J. Gilmer, J. Yosinski, and J. Sohl-Dickstein. SVCCA: Singular vector canonical correlation analysis for deep learning dynamics and interpretability. In *Advances in Neural Information Processing Systems*, pages 6076–6085, 2017.

[36] C. R. Rao. The utilization of multiple measurements in problems of biological classification. *Journal of the Royal Statistical Society. Series B (Methodological)*, 10(2):159–203, 1948.

[37] S. M. Shah. Stochastic approximation on Riemannian manifolds. *Applied Mathematics & Optimization*, pages 1–29, 2019.

[38] C. G. Snoek, M. Worring, J. C. Van Gemert, J.-M. Geusebroek, and A. W. Smeulders. The challenge problem for automated detection of 101 semantic concepts in multimedia. In *Proceedings of the 14th ACM international conference on Multimedia*, pages 421–430, 2006.

[39] K. L. Stachenfeld, M. Botvinick, and S. J. Gershman. Design principles of the hippocampal cognitive map. *Advances in neural information processing systems*, 27, 2014.

[40] V. Tan, N. Firoozye, and S. Zohren. Canonical portfolios: Optimal asset and signal combination. *arXiv preprint arXiv:2202.10817*, 2022.

[41] C. Tang. Exponentially convergent stochastic k-PCA without variance reduction. In *Advances in Neural Information Processing Systems*, pages 12393–12404, 2019.

[42] G. Tzounas, I. Dassios, M. Liu, and F. Milano. Comparison of numerical methods and open-source libraries for eigenvalue analysis of large-scale power systems. *Applied Sciences*, 10(21):7592, 2020.

[43] P. Virtanen, R. Gommers, T. E. Oliphant, M. Haberland, T. Reddy, D. Cournapeau, E. Burovski, P. Peterson, W. Weckesser, J. Bright, S. J. van der Walt, M. Brett, J. Wilson, K. J. Millman, N. Mayorov, A. R. J. Nelson, E. Jones, R. Kern, E. Larson, C. J. Carey, İ. Polat, Y. Feng, E. W. Moore, J. VanderPlas, D. Laxalde, J. Perktold, R. Cimrman, I. Henriksen, E. A. Quintero, C. R. Harris, A. M. Archibald, A. H. Ribeiro, F. Pedregosa, P. van Mulbregt, and SciPy 1.0 Contributors. SciPy 1.0: Fundamental Algorithms for Scientific Computing in Python. *Nature Methods*, 17:261–272, 2020. doi: 10.1038/s41592-019-0686-2.

[44] U. Von Luxburg. A tutorial on spectral clustering. *Statistics and Computing*, 17(4):395–416, 2007.

[45] W. Wang, J. Wang, D. Garber, and N. Srebro. Efficient globally convergent stochastic optimization for canonical correlation analysis. *Advances in Neural Information Processing Systems*, 29, 2016.

A Preliminaries: Generalized Eigenvalue Problem

The following known properties of the GEP are useful for our analysis and broadening the scope of GEP applications.

Lemma 2 (*B*-orthogonality). $v_i^\top B v_j = v_j^\top B v_i = 0$ for any distinct pair of generalized eigenvectors of $Av = \lambda Bv$ where A is symmetric and B is symmetric positive definite.

Proof. Consider the eigenvalue problem $B^{-\frac{1}{2}}AB^{-\frac{1}{2}}w = \lambda w$. Let v be a generalized eigenvector of the generalized eigenvalue problem $Av = \lambda' Bv$. Then the former eigenvalue problem is solved by $w = B^{\frac{1}{2}}v$. By inspection, $B^{-\frac{1}{2}}AB^{-\frac{1}{2}}w = B^{-\frac{1}{2}}AB^{-\frac{1}{2}}B^{\frac{1}{2}}v = B^{-\frac{1}{2}}Av = \lambda' B^{-\frac{1}{2}}Bv = \lambda' B^{\frac{1}{2}}v = \lambda' w$. Direct computation of the Rayleigh quotients for both problems reveals $\lambda = \lambda'$. Note that B is positive definite, i.e., full-rank, establishing a bijection between v and w : $v = B^{-\frac{1}{2}}w$. Also, note that $B^{-\frac{1}{2}}AB^{-\frac{1}{2}}$ is symmetric because A and B are symmetric, therefore, w may be chosen such that $W^\top W = I$ which implies $w_i^\top w_j = \delta_{ij} = v_i^\top B^{\frac{1}{2}}B^{\frac{1}{2}}v_j = v_i^\top Bv_j$, i.e., the generalized eigenvectors are B -orthogonal. \square

Proposition 3 (Similar Matrices). *Given symmetric matrices A and $B \succ 0$, consider the generalized eigenvalue problem $Av = \lambda' Bv$ with λ' and v its corresponding generalized eigenvalues and eigenvectors. Then the eigenvectors and eigenvalues of the related eigenvalue problem $B^{-\frac{1}{2}}AB^{-\frac{1}{2}}w = \lambda w$ are $w = B^{\frac{1}{2}}v$ and $\lambda = \lambda'$.*

Proof. The relationship between the eigenvectors of the two problems is proven in Lemma 2. The relationship between the eigenvalues can be proven by inspection after calculating the Rayleigh quotients for both problems:

$$\lambda' = \frac{v^\top Av}{v^\top Bv} \tag{8}$$

$$\lambda = \frac{w^\top B^{-\frac{1}{2}}AB^{-\frac{1}{2}}w}{w^\top w} \tag{9}$$

$$= \frac{v^\top B^{\frac{1}{2}}B^{-\frac{1}{2}}AB^{-\frac{1}{2}}B^{\frac{1}{2}}v}{v^\top Bv} \tag{10}$$

$$= \frac{v^\top Av}{v^\top Bv} \tag{11}$$

$$= \lambda'. \tag{12}$$

\square

A.1 Computing Subspace Error for GEP

Lemma 2 states that the generalized eigenvectors are B -orthogonal rather than orthogonal under the standard Euclidean basis. Therefore, we cannot compute subspace error in the same way as is typically done for e.g., singular value decomposition. However, we can exploit Lemma 3 to compute subspace error for the related eigenvalue problem $B^{-\frac{1}{2}}AB^{-\frac{1}{2}}w = \lambda w$ which *does* have orthogonal eigenvectors due to its symmetry.

Formally, let v be a solution to the GEP, $Av = \lambda' Bv$. Then by Lemma 3, $w = B^{1/2}v$ is a solution to $B^{-1/2}AB^{-1/2}w = \lambda w$, with eigenvalue $\lambda = \lambda'$. Leveraging this equivalence, we can measure subspace error of the GEP solution by first mapping it to the normalized case and computing subspace error there where W contains the top- k eigenvectors of $B^{-1/2}AB^{-1/2}$. Also let $\hat{W} = B^{1/2}\hat{V}$ where \hat{V} contains our top- k approximations. Given the top- k ground truth eigenvectors W and approximations \hat{W} , normalized subspace error can then be computed as $1 - \frac{1}{k} \text{tr}(U^*P) \in [0, 1]$ where $U^* = WW^\dagger$ and $P = \hat{W}\hat{W}^\dagger$ [15, 41].

B Γ -EigenGame is Well-Posed

First, we prove Γ -EigenGame suitably captures the top- k GEP.

Lemma 1 (Well-posed Utilities). *Given exact parents and assuming the top- k eigenvalues of $B^{-1}A$ are distinct and positive, the maximizer of player i 's utility is the unique generalized eigenvector v_i (up to sign, i.e., $-v_i$ is also valid).*

Proof. Assume the parents have been learned exactly and let $\hat{v}_i = \sum_p w_p v_p$ with $\|\hat{v}_i\| = 1$. Expand and simplify the following expressions that appear in the utility definition with the knowledge that the generalized eigenvectors are guaranteed to be B -orthogonal, i.e., $v_i^\top B v_j = 0$ for all $i \neq j$ (see Lemma 2 in appendix):

$$\langle \hat{v}_i, B \hat{v}_i \rangle = \left(\sum_p w_p v_p \right)^\top B \left(\sum_l w_l v_l \right) = \sum_p \sum_l w_p w_l v_p^\top B v_l = \sum_p w_p^2 \langle v_p, B v_p \rangle \quad (13)$$

$$\langle \hat{v}_i, A \hat{v}_i \rangle = \left(\sum_p w_p v_p \right)^\top A \left(\sum_l w_l v_l \right) = \sum_p \sum_l \lambda_l w_p w_l v_p^\top B v_l = \sum_p \lambda_p w_p^2 \langle v_p, B v_p \rangle \quad (14)$$

$$\langle \hat{v}_i, B v_j \rangle = \left(\sum_p w_p v_p \right)^\top B v_j = w_j \langle v_j, B v_j \rangle \quad (15)$$

$$\langle \hat{v}_i, A v_j \rangle = \left(\sum_p w_p v_p \right)^\top A v_j = \lambda_j w_j \langle v_j, B v_j \rangle. \quad (16)$$

Plugging these in to the utility function, we find

$$u_i(\hat{v}_i | v_{j < i}) = \frac{\langle \hat{v}_i, A \hat{v}_i \rangle}{\langle \hat{v}_i, B \hat{v}_i \rangle} - \sum_{j < i} \frac{\langle v_j, A v_j \rangle \langle \hat{v}_i, B v_j \rangle^2}{\langle v_j, B v_j \rangle^2 \langle \hat{v}_i, B \hat{v}_i \rangle} \quad (17)$$

$$= \frac{\langle \hat{v}_i, A \hat{v}_i \rangle}{\langle \hat{v}_i, B \hat{v}_i \rangle} - \sum_{j < i} \frac{\lambda_j \langle \hat{v}_i, B v_j \rangle^2}{\langle v_j, B v_j \rangle \langle \hat{v}_i, B \hat{v}_i \rangle} \quad \langle v_j, A v_j \rangle \rightarrow \langle v_j, \lambda_j B v_j \rangle \quad (18)$$

$$= \frac{\langle \hat{v}_i, A \hat{v}_i \rangle}{\langle \hat{v}_i, B \hat{v}_i \rangle} - \sum_{j < i} \frac{\langle \hat{v}_i, A v_j \rangle \langle \hat{v}_i, B v_j \rangle}{\langle v_j, B v_j \rangle \langle \hat{v}_i, B \hat{v}_i \rangle} \quad \langle \hat{v}_i, \lambda_j B v_j \rangle \rightarrow \langle \hat{v}_i, A v_j \rangle \quad (19)$$

$$= \frac{1}{\sum_p w_p^2 \langle v_p, B v_p \rangle} \left[\sum_l \lambda_l w_l^2 \langle v_l, B v_l \rangle - \sum_{j < i} \frac{(\lambda_j w_j \langle v_j, B v_j \rangle)(w_j \langle v_j, B v_j \rangle)}{\langle v_j, B v_j \rangle} \right] \quad (20)$$

$$= \sum_l \lambda_l z_l - \sum_{j < i} \lambda_j z_j = \sum_{j \geq i} \lambda_j z_j. \quad (21)$$

where

$$z_j = \frac{w_j^2 \langle v_j, B v_j \rangle}{\sum_p w_p^2 \langle v_p, B v_p \rangle} = \frac{w_j^2 b_j^2}{\sum_p w_p^2 b_p^2} = \frac{q_j^2}{\sum_p q_p^2} \quad (22)$$

and $z \in \Delta^{d-1}$.

This is a linear optimization problem over the simplex. Given that the eigenvalues are distinct and positive, we have that the unique solution is $z = e_i$, the onehot vector with a 1 at index i .

In order to prove uniqueness of w (up to sign), we apply Lemma 3, which proves a bijection (up to sign) between z and w , completing the proof. \square

Lemma 3. *Let $z \in \Delta^{d-1}$ such that $z_j = \frac{w_j^2 \langle v_j, B v_j \rangle}{\sum_p w_p^2 \langle v_p, B v_p \rangle}$ where w parameterizes the approximation $\hat{v}_i = \sum_p w_p v_p \in \mathcal{S}^{d-1}$. There exists a unique bijection (up to sign of w_j) between z_j and w_j , i.e., $w_j = \pm g(z)_j$.*

Proof. Let $b_j = \langle v_j, B v_j \rangle$ and $q_j = w_j b_j$ so that $w_j = q_j / b_j$. Then $\hat{v}_i = \sum_p \frac{q_p}{b_p} v_p$. Also, $q_j^2 = c z_j$ where $c = \sum_p q_p^2$ so that q_j^2 is uniquely defined up to a scalar multiple, i.e., its direction is

immediately unique by this formula but not its magnitude. Recall $\langle v_i, Bv_j \rangle = 0$ for all $i \neq j$ which implies $V^\top BV$ is diagonal. Therefore, the constraint $\|\hat{v}_i\| = \|w\|_{V^\top V}^2 = 1$ translates to $\|q\|_{V^\top V}^2 = q^\top (V^\top BV)^{-1/2} (V^\top V) (V^\top BV)^{-1/2} q = q^\top D^{-1} q = 1$. In other words, whereas an approximate eigenvector for the standard eigenvalue problem can be modeled as choosing a vector on the unit-sphere, an approximate eigenvector for the generalized eigenvalue problem is modeled as choosing a vector on an ellipsoid (D is positive definite because $V^\top V$ is symmetric positive definite assuming distinct eigenvalues, and we are given B is symmetric positive definite). This result uniquely defines a magnitude for q , therefore, combining it with the previous result uniquely defines w_j^2 from q_j^2 completing the bijection. The only degree of freedom that remains is the sign of w_j which is expected as both v_i and $-v_i$ are valid eigenvectors. \square

Although player i 's utility u_i appears abstruse, it actually has a simple explanation and structure.

Proposition 1 (Utility Shape). *Each player's utility is periodic in the angular deviation (θ) along the sphere. Its shape is sinusoidal, but with its angular axis (θ) smoothly deformed as a function of B . Most importantly, every local maximum is a global maximum (see Figure 1 for an example).*

Proof. Lemma 1 proves each utility function can be represented as a linear function over a simplex $z \in \Delta^{d-1}$. Lemma 3 then proves this simplex can be parameterized by a variable q constrained to an ellipsoid with curvature $D = \text{diag}(\dots, \langle v_i, Bv_i \rangle, \dots)$. This matches the analysis of EigenGame exactly, except that $D = I$ in that previous work. The implication is that each utility function as defined in equation (5) is also a cosine, but with its angular axis deformed according to D . \square

As an example consider setting

$$A = \begin{bmatrix} 0.77759061 & 0.26842584 \\ 0.26842584 & 0.87788983 \end{bmatrix} \quad B = \begin{bmatrix} 0.2325605 & 0.06042127 \\ 0.06042127 & 0.03241424 \end{bmatrix} \quad (23)$$

and observe the utilities in Figure 1.

Our proposed utilities tie nicely back to previous work [16] via their gradients and our derived update directions.

Proposition 4 (Equivalence to EigenGame Unloaded). *The Generalized EigenGame pseudogradient in equation (12) is equivalent to the Riemannian gradient in [15] when $B = I$.*

Proof. In order to compute the Riemannian update direction, we project player i 's direction onto the tangent space of the unit-sphere by left-multiplying with $(I - \hat{v}_i \hat{v}_i^\top)$. Starting with equation (12), we find

$$\tilde{v}_i = \overbrace{(\hat{v}_i^\top B \hat{v}_i) A \hat{v}_i - (\hat{v}_i^\top A \hat{v}_i) B \hat{v}_i}^{\text{reward}} - \sum_{j < i} \overbrace{(\hat{v}_i^\top A \hat{v}_j) [\langle \hat{v}_i, B \hat{v}_i \rangle B \hat{v}_j - \langle \hat{v}_i, B \hat{v}_j \rangle B \hat{v}_i]}^{\text{penalty}} \quad (24)$$

$$= A \hat{v}_i - (\hat{v}_i^\top A \hat{v}_i) \hat{v}_i - \sum_{j < i} (\hat{v}_i^\top A \hat{v}_j) [\hat{v}_j - \langle \hat{v}_i, \hat{v}_j \rangle \hat{v}_i] \quad (25)$$

$$= (I - \hat{v}_i \hat{v}_i^\top) [A \hat{v}_i - \sum_{j < i} (\hat{v}_i^\top A \hat{v}_j) \hat{v}_j] = (I - \hat{v}_i \hat{v}_i^\top) \tilde{\nabla}_i^{\mu-EG}. \quad (26)$$

\square

C Smooth and Unbiased

In order to prove asymptotic convergence of γ -EigenGame in the deterministic setting, we establish the following lemmas.

Lemma 4. *The update $\tilde{\nabla}_i$ in equation (7) is smooth.*

Proof. The reward terms are polynomial in \hat{v}_i and therefore smooth (analytic). The numerators of the penalty terms are also polynomial in \hat{v}_i and \hat{v}_j , however, the denominator includes a scalar $\langle \hat{v}_j, B\hat{v}_j \rangle$. Given $B \succ 0$, this term is guaranteed to be greater than the minimum eigenvalue of B (which is positive), thereby ensuring the penalty terms are non-singular. So these terms are also smooth. \square

Instead of proving the following lemmas directly for Algorithm 1 (the deterministic variant), we prove them for Algorithm 2, which subsumes Algorithm 1 ($\rho = 0, \gamma_t = 1, b = n, M = 1$).

The following two lemmas are proven in the single proof below.

Lemma 5. *The unique stable fixed point (up to sign of \hat{v}_j) of Algorithm 2 run with exact expectations (e.g., $n' = n$ where n is the full dataset size) is $\hat{v}_j = v_j$ for all $j \in \{1, \dots, k\}$, i.e., the top- k generalized eigenvectors.*

Lemma 6. *Algorithm 2's updates are asymptotically unbiased.*

Proof. The proof is constructed sequentially by proving each update process has a unique stable fixed point conditioned on the previous updates' fixed points defined by the hierarchy imposed on the players. We explain how we are able to address constructing unbiased estimates of each update as well, thereby supporting a stochastic, asymptotic convergence proof.

The proof begins by considering the updates of the first player on \hat{v}_1 . Player 1 is unique in that it pays no penalties for aligning with other players. Its update consists of the reward terms only, which comprises an unbiased estimate assuming independent, unbiased estimates for A and B (i.e., these are constructed with independent minibatches). Player 1's update simply performs Riemannian gradient ascent on its utility function. Proposition 1 proves that every maximum of this function is a global maximum (in addition, it contains no saddle points). Therefore, the only stable fixed point for \hat{v}_1 is v_1 .

Next, we consider player 1's update to $[B\hat{v}]_1$. Given we just showed \hat{v}_1 's stable fixed point is v_1 , and this update is simply a running average, its unique stable fixed point is Bv_1 .

We now consider player 2's update, which includes penalty terms. Plugging $[B\hat{v}]_1$'s unique stable fixed point into these penalty terms, and again assuming independent, unbiased estimates for A and B , allows us to construct an unbiased estimate of the penalty terms. Similarly to player 1's analysis, player 2's update performs Riemannian gradient ascent on a utility function with a unique stable fixed point, $\hat{v}_2 = v_2$.

The proof then proceeds repeating the same arguments, alternating between proving the unique stable fixed point of each $[B\hat{v}]_j = Bv_j$ and $\hat{v}_j = v_j$. \square

D Error Propagation

An error propagation analysis is necessary to rule out the scenario where an arbitrary (unbounded) level of precision is required by the parents to ensure any progress towards the true solution can be made by the children. In other words, we show that as the parents near their true solutions, the children may near theirs as well.

As before in Appx. C, we will perform this analysis for the stochastic version of the algorithm (Algorithm 2), but note that this subsumes the analysis for the deterministic version (where $[B\hat{v}]_j$ is replaced by the exact Bv_j with zero error).

Player 1's update of \hat{v}_1 is unbiased without any assumptions on the state of any of the other player vectors $\hat{v}_{j>1}$ or auxiliary variables $[B\hat{v}]_{j \geq 1}$. We would like to understand how transient error in \hat{v}_1 propagates through to these other variables. The updates of player 1's children depend on $[B\hat{v}]_1$, so we analyze the effect on it first. Note that the error propagation analysis naturally repeats as we progress down the hierarchy of players, so we analyze how error in \hat{v}_i propagates through to $[B\hat{v}]_i$ and then onto $\hat{v}_{j>i}$. Interestingly, step 2 of the following proof suggests the error in the \hat{v}_i must fall below $\frac{1}{\kappa}$ before any increase in accuracy of the

parents helps to improve accuracy in the children. This result mirrors that of [15] (see their Appendix F).

Theorem 3. *An $\mathcal{O}(\epsilon)$ angular error in the parent propagates to an $\mathcal{O}(\epsilon^{\frac{1}{2}})$ upper bound on the angular error of the child's solution.*

Proof. The proof proceeds in three steps:

1. $\mathcal{O}(\epsilon)$ angular error of parent $v_i \implies \mathcal{O}(\epsilon)$ Euclidean error of parent v_i
2. $\mathcal{O}(\epsilon)$ Euclidean error of parent $v_i \implies \mathcal{O}(\epsilon)$ Euclidean error of norm of child $v_{j>i}$'s gradient
3. $\mathcal{O}(\epsilon)$ Euclidean error of norm child $v_{j>i}$'s gradient + instability of minima at $v_{k \neq j} \implies \mathcal{O}(\epsilon)$ angular error of child $v_{j>i}$'s solution assuming $B = I$.
4. $\mathcal{O}(\epsilon)$ angular error of child $v_{j>i}$'s solution assuming $B = I \implies \mathcal{O}(\epsilon^{\frac{1}{2}})$ angular error of child $v_{j>i}$'s solution for a general $B \succ 0$.

1. As in μ -EigenGame, an *angular error* of ϵ in the parent translates to ϵ *Euclidean error*. The proof is exactly the same as in [15], repeated here for convenience. Angular error in the parent can be converted to Euclidean error by considering the chord length between the mis-specified parent and the true parent direction. The two vectors plus the chord form an isosceles triangle with the relation that chord length $l = 2 \sin(2\epsilon)$ is $\mathcal{O}(\epsilon)$ for $\epsilon \ll 1$.

2. Next, write the mis-specified parents as $\hat{v}_i = v_i + w_i$ where $\|w_i\|$ is $\mathcal{O}(\epsilon_i)$ as we just explained.

Now consider the fixed point of the auxiliary variable's update: $[Bv]_i = B(v_i + w_i) = Bv_i + Bw_i$. Hence any mis-specification in the parent \hat{v}_i appears as a mis-specification of the auxiliary variable's fixed point by Bw_i , which is $\mathcal{O}(\lambda_{\max}\epsilon)$ where λ_{\max} is the maximum eigenvalue (spectral radius) of B . Assume the auxiliary variable is mis-specified by an additional error (q_i where $\|q_i\|$ is $\mathcal{O}(\epsilon'_i)$) representing failure to precisely reach the perturbed fixed point $B(v_i + w_i)$, i.e., $[B\hat{v}]_i = B(v_i + w_i) + q_i$.

The auxiliary variable impacts the update of $\hat{v}_{j>i}$ through \hat{y}_i and similarly $[B\hat{y}]_i$:

$$\hat{y}_i = \frac{\hat{v}_i}{\sqrt{[\langle \hat{v}_i, [B\hat{v}]_i \rangle]_\rho}} \quad (27)$$

$$= \frac{v_i + w_i}{\sqrt{[\langle \hat{v}_i, Bv_i \rangle + \langle \hat{v}_i, Bw_i \rangle + \langle \hat{v}_i, q_i \rangle]_\rho}} \quad (28)$$

$$= \frac{v_i + w_i}{\sqrt{[\langle v_i, Bv_i \rangle + 2\langle v_i, Bw_i \rangle + \langle w_i, Bw_i \rangle + \langle v_i, q_i \rangle + \langle w_i, q_i \rangle]_\rho}} \quad (29)$$

$$= cy_i + \frac{w_i}{\sqrt{[\langle v_i, Bv_i \rangle + 2\langle v_i, Bw_i \rangle + \langle w_i, Bw_i \rangle + \langle v_i, q_i \rangle + \langle w_i, q_i \rangle]_\rho}} \quad (30)$$

$$= cy_i + e_i \quad (31)$$

In order to bound this term, we make a few mild assumptions.

- Assume ρ is less than λ_{\min} as stated earlier and, in particular, less than the lower bound.
- Assume ϵ'_i is $\mathcal{O}(\epsilon_i)$ to ease the exposition.
- Also, w.l.o.g., assume $\lambda_{\max} > 1$; if not, we can simply scale the problem such that it is true.

Let $\kappa = \frac{\lambda_{\max}}{\lambda_{\min}}$ be the condition number of B , and note that the error term in the denominator is bounded by the spectrum of B :

$$\lfloor \langle \hat{v}_i, [B\hat{v}]_i \rangle \rfloor_{\rho} \leq \langle v_i, Bv_i \rangle + 2\lambda_{\max}\epsilon_i + \lambda_{\max}\epsilon_i^2 + \epsilon'_i + \epsilon_i\epsilon'_i \quad (32)$$

$$\underbrace{\leq}_{1 \leq \lambda_{\max} \leq \kappa \langle v_i, Bv_i \rangle} \langle v_i, Bv_i \rangle (1 + 2\kappa\epsilon_i + \kappa\epsilon_i^2 + \kappa\epsilon'_i + \kappa\epsilon_i\epsilon'_i) \quad (33)$$

$$\underbrace{\leq}_{\epsilon' \text{ is } \mathcal{O}(\epsilon)} \langle v_i, Bv_i \rangle (1 + 3\kappa\epsilon_i + 2\kappa\epsilon_i^2) \quad (34)$$

and vice versa for the lower bound, which implies

$$(35)$$

$$\lfloor \langle \hat{v}_i, [B\hat{v}]_i \rangle \rfloor_{\rho} \in \langle v_i, [Bv]_i \rangle \left[(1 - 3\kappa\epsilon_i - 2\kappa\epsilon_i^2), (1 + 3\kappa\epsilon_i + 2\kappa\epsilon_i^2) \right]. \quad (36)$$

Then

$$c \in \left[\frac{1}{\sqrt{1 + 3\kappa\epsilon_i + 2\kappa\epsilon_i^2}}, \frac{1}{\sqrt{1 - 3\kappa\epsilon_i - 2\kappa\epsilon_i^2}} \right]. \quad (37)$$

Note that if $\epsilon_i \ll \frac{1}{\kappa}$, then c is $\mathcal{O}(1)$. Note this condition also implies e_i is $\mathcal{O}(\epsilon'_i)$. We will use these facts later.

Now we are prepared to consider the norm of the difference, d_j , between the Riemannian⁵ update to \hat{v}_j with exact parents and auxiliary variables versus the actual inexact Riemannian update. Let Δ_j^R be defined as in line 12 of Algorithm 2. Define $\bar{\Delta}_j^R$ to be the same except with \hat{y}_l and $[B\hat{y}]_l$ terms replaced by their true solution counterparts y_l and $[By]_l$. Note that Δ_j^R and $\bar{\Delta}_j^R$ already live in the tangent space of the unit-sphere at \hat{v}_j . Then the norm of the difference between the two update directions is upper bounded as

$$\|d_j\| = \|\Delta_j^R - \bar{\Delta}_j^R\| \quad (38)$$

$$\leq \left\| \sum_{l < i} \left[(\hat{v}_j^\top A\hat{y}_l) [\langle \hat{v}_j, B\hat{v}_j \rangle [B\hat{y}]_l - \langle \hat{v}_j, [B\hat{y}]_l \rangle B\hat{v}_j] - \dots \right] \right\| \quad (39)$$

$$\leq \sum_{l < i} \left\| \left[(\hat{v}_j^\top A\hat{y}_l) [\langle \hat{v}_j, B\hat{v}_j \rangle [B\hat{y}]_l - \langle \hat{v}_j, [B\hat{y}]_l \rangle B\hat{v}_j] - \dots \right] \right\|. \quad (40)$$

Recall q_i is the error associated with suboptimality of $[B\hat{v}]_i$ and propagates to $[B\hat{y}]_i$ as defined on line 9 of Algorithm 2. Let

$$p_i = \frac{q_i}{\sqrt{\lfloor \langle v_i, Bv_i \rangle + 2\langle v_i, Bw_i \rangle + \langle w_i, Bw_i \rangle + \langle v_i, q_i \rangle + \langle w_i, q_i \rangle \rfloor_{\rho}}}. \quad (41)$$

By similar arguments used to bound e_i , $\|p_i\|$ is $\mathcal{O}(\epsilon'_i)$ if $\epsilon_i \ll \frac{1}{\kappa}$.

Bounding the summand in equation (40), we find

$$\|(\hat{v}_j^\top A\hat{y}_l) [\langle \hat{v}_j, B\hat{v}_j \rangle [B\hat{y}]_l - \langle \hat{v}_j, [B\hat{y}]_l \rangle B\hat{v}_j] - (\hat{v}_j^\top A y_l) [\langle \hat{v}_j, B\hat{v}_j \rangle [By]_l - \langle \hat{v}_j, [By]_l \rangle B\hat{v}_j]\| \quad (42)$$

$$= \|(c\hat{v}_j^\top A y_l + \hat{v}_j^\top A e_l) [\langle \hat{v}_j, B\hat{v}_j \rangle (cBy_l + Be_l + p_l) - \langle \hat{v}_j, (cBy_l + Be_l + p_l) \rangle B\hat{v}_j] - \dots\| \quad (43)$$

$$= \|(c^2 - 1)(\hat{v}_j^\top A y_l) [\langle \hat{v}_j, B\hat{v}_j \rangle By_l - \langle \hat{v}_j, By_l \rangle B\hat{v}_j] + \mathcal{O}(\epsilon)\|. \quad (44)$$

Recall equation (37) and note that

$$c^2 - 1 \in \left\{ \frac{-3\kappa\epsilon_i - 2\kappa\epsilon_i^2}{1 + 3\kappa\epsilon_i + 2\kappa\epsilon_i^2}, \frac{3\kappa\epsilon_i + 2\kappa\epsilon_i^2}{1 - 3\kappa\epsilon_i - 2\kappa\epsilon_i^2} \right\} \quad (45)$$

which has norm $|c^2 - 1| = \mathcal{O}(\kappa\epsilon_i)$. Therefore, taking into account the impact of the other A and B terms, $\|d_j\|$ is upper bounded by $\mathcal{O}(i\kappa\sigma(A)\lambda_{\max}^2\epsilon_i)$ where $\sigma(A)$ is the spectral radius of A .

⁵The Riemannian update projects the vanilla update onto the tangent space of the sphere.

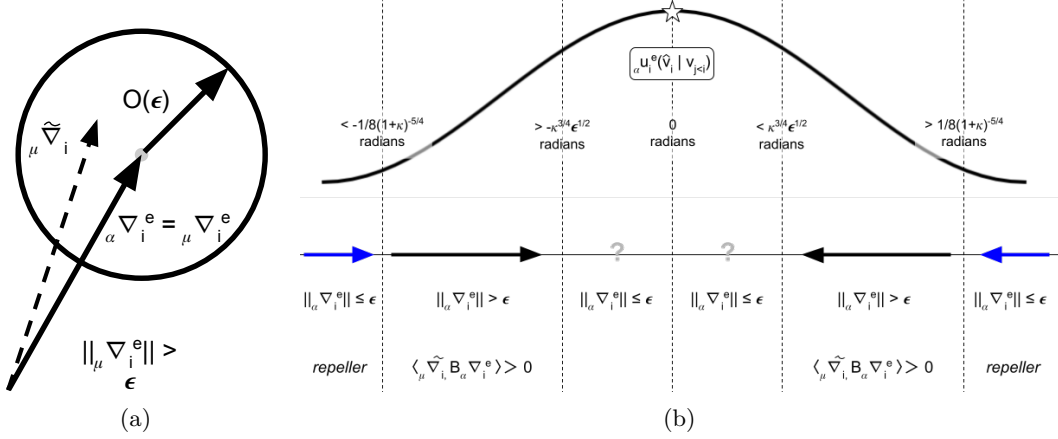


Figure 6: (a) Close in Euclidean distance can imply close in angular distance if the vectors are long enough (reprinted with permission from [15]). (b) The stable region may consist of an $\mathcal{O}(\kappa^{3/4} \epsilon^{1/2})$ ball around the true optimum as $\epsilon \rightarrow 0$.

3. We can reuse the analysis of [15] to understand how a change in the norm of the vector field relates to a change in the location of the fixed point. This is because the Riemannian update direction of our proposed method with exact parents and $B = I$ is equivalent to the Riemannian update direction in [15] (simply left-multiply their equation (4) by $(I - \hat{v}_i \hat{v}_i^\top)$ to compute their Riemannian update). Therefore, as in this prior work, an error in the gradient norm translates to the same order of error in angular distance to the true fixed point (inflated by a finite scaling dependent on the spectrum of B —accounted for in Step 4 next).

Also, the region around any generalized eigenvector $v_{l \neq j}$ is unstable and this is because the Riemannian Hessian at that point is positive (this implies instability because we are maximimizing). We can reason that the Riemannian Hessian is positive by appealing to the fact that the Riemannian Hessian of our generalized EVP utilities is related to the Hessian of prior work by a warping defined by the positive definite matrix B (for a visual, see Figure 1; for math, see Lemmas 1 and 3).

In contrast to this prior work, the generalized eigenvectors are more generally, B -orthogonal (see Lemma 2). By Lemma 7, the angular distance between generalized eigenvectors is finite and depends on the condition number of B . Therefore, there exists a small enough ϵ such that an ϵ -ball around any *unstable* region and an ϵ -ball around the *stable* region no longer overlap.

4. Lastly, Lemma 8 proves that an $\epsilon_i < 1$ angular error assuming $B = I$ can be increased to at most $\kappa^{3/4} \epsilon_i^{1/2}$ if B is relaxed to be any symmetric positive definite matrix with condition number κ . \square

Lemma 7. *The angle between a pair of orthonormal vectors when instead measured under a general positive definite matrix C is lower bounded by $\frac{1}{8}(1+\kappa)^{-5/4}$ where κ is the condition number of C , i.e., if $\langle v_i, v_j \rangle = 0$, then $|\theta| = \arccos\left(\frac{|\langle C^{\frac{1}{2}} v_i, C^{\frac{1}{2}} v_j \rangle|}{\|C^{\frac{1}{2}} v_i\| \|C^{\frac{1}{2}} v_j\|}\right) > \frac{1}{8}(1+\kappa)^{-5/4}$ radians.*

Proof. The angle between two vectors is a function of their relation to each other in the two-dimensional plane defined by their pair. Therefore, without loss of generality, consider two vectors $u = \begin{bmatrix} 1 & 0 \end{bmatrix}$ and $v = \begin{bmatrix} 0 & 1 \end{bmatrix}$ and consider the effect of an arbitrary positive definite matrix \hat{C} on their angle. For ease of exposition, denote $\tau = \kappa^{1/2}$ the condition number of $C^{\frac{1}{2}}$.

Let $\hat{C}^{\frac{1}{2}} = \begin{bmatrix} a & c \\ c & b \end{bmatrix}$ be the unique positive definite square root of \hat{C} where a and b are positive

and the determinant $ab - c^2 > \gamma > 0$. We aim to show that the magnitude of the angle between u and v under the generalized inner product $\langle \cdot, \cdot \rangle_C$ is lower bounded by a finite, positive quantity dependent on the properties of C .

Consider

$$\hat{C}^{\frac{1}{2}}u = \begin{bmatrix} a \\ c \end{bmatrix}, \quad \hat{C}^{\frac{1}{2}}v = \begin{bmatrix} c \\ b \end{bmatrix}, \quad (46)$$

$$\|\hat{C}^{\frac{1}{2}}u\| = \sqrt{a^2 + c^2}, \quad \|\hat{C}^{\frac{1}{2}}v\| = \sqrt{c^2 + b^2}, \quad (47)$$

$$\langle \hat{C}^{\frac{1}{2}}u, \hat{C}^{\frac{1}{2}}v \rangle = c(a + b). \quad (48)$$

Then

$$\frac{\langle \hat{C}^{\frac{1}{2}}u, \hat{C}^{\frac{1}{2}}v \rangle}{\|C^{\frac{1}{2}}u\| \|C^{\frac{1}{2}}v\|} = \frac{c(a + b)}{\sqrt{(a^2 + c^2)(c^2 + b^2)}} \quad (49)$$

$$\overbrace{<}^{\text{ratio is inc. in } c \text{ for } ab > c^2} \frac{\sqrt{ab - \gamma}(a + b)}{\sqrt{(a^2 + ab - \gamma)(ab + b^2 - \gamma)}} \quad (50)$$

$$\overbrace{=}^{\text{div. num. \& den. by } \frac{1}{a^2}} \frac{\sqrt{\frac{b}{a} - \frac{\gamma}{a^2}}(1 + \frac{b}{a})}{\sqrt{(1 + \frac{b}{a} - \frac{\gamma}{a^2})(\frac{b}{a} + (\frac{b}{a})^2 - \frac{\gamma}{a^2})}} \quad (51)$$

$$\overbrace{\leq}^{\text{ratio is inc. in } \frac{b}{a}} \frac{\sqrt{\tau - \frac{\gamma}{a^2}}(1 + \tau)}{\sqrt{(1 + \tau - \frac{\gamma}{a^2})(\tau + \tau^2 - \frac{\gamma}{a^2})}} \quad (52)$$

$$\overbrace{<}^{\text{ratio is inc. in } \tau - \frac{\gamma}{a^2}} \frac{\sqrt{\tau - \frac{\gamma}{tr^2}}(1 + \tau)}{\sqrt{(1 + \tau - \frac{\gamma}{tr^2})(\tau + \tau^2 - \frac{\gamma}{tr^2})}}. \quad (53)$$

Note that $\frac{b}{a}$ is a lower bound on the condition number of \hat{C} ; $\frac{b}{a}$ is equal to the condition number of $\hat{C}^{\frac{1}{2}}$ when $c = 0$ (assuming $b > a$, otherwise, $\frac{b}{a} < \frac{a}{b}$ clearly), and the condition number can only increase as c deviates from 0. Lastly, note that the condition number of $\hat{C}^{\frac{1}{2}}$ is upper bounded by τ , the condition number of $C^{\frac{1}{2}}$. Recall, by replacing $\frac{b}{a}$ with a larger number τ and $\frac{\gamma}{a^2}$ with a strictly smaller number $\frac{\gamma}{tr^2}$, $\frac{b}{a} - \frac{\gamma}{a^2}$ implies that $\tau > \frac{\gamma}{tr^2}$.

Now consider

$$\left(\frac{\langle C^{\frac{1}{2}}u, C^{\frac{1}{2}}v \rangle}{\|C^{\frac{1}{2}}u\| \|C^{\frac{1}{2}}v\|} \right)^2 < \frac{(\tau - \frac{\gamma}{tr^2})(1 + \tau)^2}{(1 + \tau - \frac{\gamma}{tr^2})(\tau + \tau^2 - \frac{\gamma}{tr^2})} \quad (54)$$

$$= \frac{(\tau - \frac{\gamma}{tr^2})(1 + \tau)^2}{(\tau - \frac{\gamma}{tr^2})(1 + \tau)^2 + (\frac{\gamma}{tr^2})^2} \quad (55)$$

$$= 1 - \frac{(\frac{\gamma}{tr^2})^2}{(\tau - \frac{\gamma}{tr^2})(1 + \tau)^2 + (\frac{\gamma}{tr^2})^2} \quad (56)$$

$$\leq 1 - \frac{(\frac{\gamma}{tr^2})^2}{(\tau)(1 + \tau)^2 + (1 + \tau)^2} \quad (57)$$

$$= 1 - \frac{(\frac{\gamma}{tr^2})^2}{(1 + \tau)^3}. \quad (58)$$

We can also simplify the fraction $\frac{\gamma}{tr^2}$. γ is a lower bound on the determinant, which is equal to the product of eigenvalues of $\hat{C}^{\frac{1}{2}}$. This is lower bounded by λ_{min}^2 for any two-dimensional

subspace, therefore, $\lambda_{min}^2 < \gamma$. Furthermore, the trace of the matrix is equal to the sum of its eigenvalues. This is upper bounded by $2\lambda_{max}$ for any two-dimensional subspace, therefore $\frac{\gamma}{tr^2} > \frac{\lambda_{min}^2}{4\lambda_{max}^2} = \frac{1}{4\tau^2} > \frac{1}{4(\tau+1)^2}$.

Note that $|\theta| \geq |\sin(\theta)|$. Therefore,

$$|\theta| \geq |\sin(\theta)| = \sqrt{1 - \cos^2(\theta)} \quad (59)$$

$$> \sqrt{\frac{(\frac{\gamma}{tr^2})^2}{(1+\tau)^3}} \quad (60)$$

$$> \frac{1}{2} \sqrt{(1+\tau)^{-5}} \quad (61)$$

$$= \frac{1}{2} (1+\tau)^{-\frac{5}{2}}. \quad (62)$$

Clearly this bound is loose as it implies θ is only greater than $2^{-\frac{7}{2}}$ for $C = I$ ($\tau = 1$) whereas we know in that case that $\theta = \frac{\pi}{2}$. However, this bound serves its purpose of establishing a finite impact of C on the orthogonality of the original two vectors, i.e., if u and v are orthogonal, their angle as measured under a generalized inner product by $C \succ 0$ cannot be 0.

Replacing τ with $\kappa^{\frac{1}{2}}$, we can further simplify the bound to

$$|\theta| > \frac{1}{2} (1+\tau)^{-\frac{5}{2}} \quad (63)$$

$$\geq \frac{1}{8} (1+\kappa)^{-\frac{5}{4}}. \quad (64)$$

□

Lemma 8. *The angle between a pair of nearly parallel vectors ($|\theta|$ is $\mathcal{O}(\epsilon)$ with $\epsilon \ll 1$) when instead measured under a general positive definite matrix C is upper bounded by $\mathcal{O}(\kappa^{\frac{3}{4}}\epsilon^{\frac{1}{2}})$.*

Proof. Let $C^{\frac{1}{2}} = \begin{bmatrix} a & c \\ c & b \end{bmatrix}$ be the unique positive definite square root of C where a and b are positive and the determinant $ab - c^2 > 0$. Consider a vector $u = \begin{bmatrix} 1 & 0 \end{bmatrix}$ and another vector $v = \begin{bmatrix} \sqrt{1-\epsilon^2} & \epsilon \end{bmatrix}$ that is nearly parallel to u , i.e., $\epsilon \ll 1$ (implies $|\theta|$ is $\mathcal{O}(\epsilon)$). We aim to show that the angle between these two vectors under the generalized inner product $\langle \cdot, \cdot \rangle_C$ is upper bounded by a constant multiple of ϵ given a small enough ϵ .

Consider

$$C^{\frac{1}{2}}u = \begin{bmatrix} a \\ c \end{bmatrix}, \quad C^{\frac{1}{2}}v = \begin{bmatrix} a\sqrt{1-\epsilon^2} + c\epsilon \\ c\sqrt{1-\epsilon^2} + b\epsilon \end{bmatrix}, \quad (65)$$

$$\|C^{\frac{1}{2}}u\| = \sqrt{a^2 + c^2} \quad (66)$$

$$= a\sqrt{1 + (c/a)^2}, \quad (67)$$

$$= a\sqrt{1 + (c/a)^2 + \epsilon^2(b^2 - a^2)}, \quad (68)$$

and

$$\langle C^{\frac{1}{2}}u, C^{\frac{1}{2}}v \rangle = a^2\sqrt{1-\epsilon^2} + ace + c^2\sqrt{1-\epsilon^2}bce \quad (69)$$

$$= (a^2 + c^2)\sqrt{1-\epsilon^2} + (a+b)c\epsilon \quad (70)$$

$$= a^2(1 + (c/a)^2)\sqrt{1-\epsilon^2} + a^2(1 + (b/a))(c/a)\epsilon \quad (71)$$

$$\underbrace{\geq a(1 + (c/a)^2)(1 - \epsilon^2) + a^2(1 + (b/a))(c/a)\epsilon}_{|\epsilon| < 1}. \quad (72)$$

Then

$$\frac{\langle C^{\frac{1}{2}}u, C^{\frac{1}{2}}v \rangle}{\|C^{\frac{1}{2}}u\| \|C^{\frac{1}{2}}v\|} \geq \frac{(1 + (c/a)^2)(1 - \epsilon^2) + (1 + (b/a))(c/a)\epsilon}{(1 + (c/a)^2)\sqrt{1 + \epsilon^2 \frac{(b/a)^2 - 1}{(c/a)^2 + 1}}} \quad (73)$$

$$= \frac{1}{\sqrt{1 + \epsilon^2 \frac{(b/a)^2 - 1}{(c/a)^2 + 1}}} + \frac{(1 + (b/a))(c/a)\epsilon - (1 + (c/a)^2)\epsilon^2}{(1 + (c/a)^2)\sqrt{1 + \epsilon^2 \frac{(b/a)^2 - 1}{(c/a)^2 + 1}}} \quad (74)$$

$$\overset{b/a \leq \kappa}{\geq} \frac{1}{\sqrt{1 + \epsilon^2 \kappa^2}} + \frac{(1 + (b/a))(c/a)\epsilon - (1 + (c/a)^2)\epsilon^2}{(1 + (c/a)^2)\sqrt{1 + \epsilon^2 \frac{(b/a)^2 - 1}{(c/a)^2 + 1}}} \quad (75)$$

$$= 1 - (1 - \frac{1}{\sqrt{1 + \epsilon^2 \kappa^2}}) + \frac{(1 + (b/a))(c/a)\epsilon - (1 + (c/a)^2)\epsilon^2}{(1 + (c/a)^2)\sqrt{1 + \epsilon^2 \frac{(b/a)^2 - 1}{(c/a)^2 + 1}}} \quad (76)$$

$$\overset{c \geq -\sqrt{ab}}{\geq} 1 - (1 - \frac{1}{\sqrt{1 + \epsilon^2 \kappa^2}}) - \frac{(1 + (b/a))\sqrt{(b/a)}|\epsilon| - (1 + (c/a)^2)\epsilon^2}{(1 + (c/a)^2)\sqrt{1 + \epsilon^2 \frac{(b/a)^2 - 1}{(c/a)^2 + 1}}} \quad (77)$$

$$= 1 - (1 - \frac{1}{\sqrt{1 + \epsilon^2 \kappa^2}}) - \frac{(1 + (b/a))\sqrt{(b/a)}|\epsilon|}{(1 + (c/a)^2)\sqrt{1 + \epsilon^2 \frac{(b/a)^2 - 1}{(c/a)^2 + 1}}} - \frac{\epsilon^2}{\sqrt{1 + \epsilon^2 \frac{(b/a)^2 - 1}{(c/a)^2 + 1}}} \quad (78)$$

$$\overset{b/a \leq \kappa}{\geq} 1 - (1 - \frac{1}{\sqrt{1 + \epsilon^2 \kappa^2}}) - \frac{(1 + \kappa)\sqrt{\kappa}|\epsilon|}{\sqrt{1 - \epsilon^2}} - \frac{\epsilon^2}{\sqrt{1 - \epsilon^2}} \quad (79)$$

$$\overset{1 - \frac{1}{\sqrt{1 + \epsilon^2}} \leq \frac{\kappa}{2}, \epsilon^2 < \frac{1}{\kappa^2}}{\geq} 1 - \frac{\epsilon^2}{2}\kappa^2 - \frac{(1 + \kappa)\sqrt{\kappa}|\epsilon|}{\sqrt{1 - \epsilon^2}} - \frac{\epsilon^2}{\sqrt{1 - \epsilon^2}} \quad (80)$$

$$\overset{\epsilon < \frac{1}{2}}{\geq} 1 - 2(1 + \kappa)\sqrt{\kappa}|\epsilon| - \frac{\epsilon^2}{2}(\kappa^2 - 1) - 2\epsilon^2. \quad (81)$$

Note that $\cos(\theta) \leq 1 - \frac{1}{8}\theta^2$ for $|\theta| \leq \pi$. Then

$$|\theta| \leq 2\sqrt{2}\sqrt{1 - \cos(\theta)} \leq 2\sqrt{2}\sqrt{2(1 + \kappa)\sqrt{\kappa}|\epsilon| + (\frac{\kappa^2}{2} + 2)\epsilon^2} \quad (82)$$

$$\leq 4\sqrt{(1 + \kappa)\sqrt{\kappa}|\epsilon| + (\frac{\kappa^2}{4} + 1)\epsilon^2}. \quad (83)$$

Therefore, for $\epsilon < \min(\frac{1}{\kappa}, \frac{1}{2})$, $\arccos(\frac{|\langle C^{\frac{1}{2}}u, C^{\frac{1}{2}}v \rangle|}{\|C^{\frac{1}{2}}u\| \|C^{\frac{1}{2}}v\|})$ is upper bounded by $\mathcal{O}(\epsilon^{\frac{1}{2}}\kappa^{\frac{3}{4}})$. \square

E Asymptotic Convergence

We carryout a proof of convergence of Algorithm 1 in the deterministic setting and a partial proof of Algorithm 2 with further discussion.

E.1 Asymptotic Convergence of Deterministic Update

We now give the convergence proof of Algorithm 1 using the theoretical results established above.

Theorem 2 (Deterministic / Full-batch Global Convergence). *Given a symmetric matrix A and symmetric positive definite matrix B where the top- k eigengaps of $B^{-1}A$ are positive*

along with a square-summable, not summable step size sequence η_t (e.g., $1/t$), Algorithm 1 converges to the top- k eigenvectors asymptotically ($\lim_{T \rightarrow \infty}$) with probability 1.

Proof. Assume none of the \hat{v}_i are initialized to an angle exactly at the minimum of their utility. This is a set of vectors with Lebesgue measure 0, therefore, the assumption holds w.p.1.

Denote the “update field” $H(\hat{V})$ to match the work of [37]. $H(\hat{V})$ is simply the concatenation of all players’ Riemannian update rules, i.e., all players updating in parallel using their Riemannian updates:

$$H(\hat{V}) = [\Delta_1, \dots, \Delta_k] : \mathbb{R}^{kd} \rightarrow \mathbb{R}^{kd} \quad (84)$$

where Δ_i is defined in equation (7) and \hat{V} represents the set of all \hat{v}_i .

A Riemannian gradient ascent step (with retractions) is then given by the following update step:

$$\hat{V}(t+1) \leftarrow \hat{V}(t) + \eta_t H(\hat{V}(t)) \quad (85)$$

$$\hat{v}_i(t+1) \leftarrow \hat{v}_i(t+1) / \|\hat{v}_i(t+1)\| \quad \forall i. \quad (86)$$

By Lemma 5, v_1 is the unique fixed point of \hat{v}_1 ’s update. And by Theorem 3, convergence of v_1 to within $\mathcal{O}(\epsilon)$ of its fixed point contributes to a mis-specification of children $\hat{v}_{j>1}$ ’s fixed point by $\mathcal{O}(\sqrt{\epsilon})$. Critically, this mis-specification is shrinking in ϵ so that as \hat{v}_1 nears its fixed point, so may its children. This chain of reasoning applies for all \hat{v}_i .

The result is then obtained by applying Theorem 7 of Shah [37] with the following information: **A0**) the unit-sphere is a compact manifold with an injectivity radius of π which implies the injectivity radius of the manifold of the game (the product space of k unit-spheres) is also finite, **A1**) the update field is smooth (analytic) by Lemma 4, **A2**) we assume a square-summable, not summable step size, **A3**) we assume the full-batch (noiseless) setting so the update “noise” clearly constitutes a bounded martingale difference sequence, and **A4**) the iterates remain bounded because they are constrained to the unit-sphere.

Formally, for any $T > 0$,

$$\lim_{s \rightarrow \infty} \sup_{t \in [s, s+T]} d(\hat{V}(t), \hat{V}^s(t)) \rightarrow a.s., \quad (87)$$

where $d(\cdot, \cdot)$ is the Riemannian distance on the (product space of) sphere and $\hat{V}^s(t)$ denotes the continuous time trajectory of $H(\hat{V})$ starting from $\hat{V}(s)$. \square

E.2 Asymptotic Convergence of Stochastic Update

There are two primary issues with extending the asymptotic convergence guarantee in Theorem 2 to Algorithm 2. The first is that the joint parameter space includes $\hat{v}_i \in \mathcal{S}^{d-1}$ and $[B\hat{v}]_i \in \mathbb{R}^d$. The unit-sphere, \mathcal{S}^{d-1} , is a compact Riemannian manifold. While \mathbb{R}^d is a Riemannian manifold, it is not compact. This violates assumptions **A0** and **A4** above. The second issue is that the vector field $H(\hat{V}; [B\hat{V}])$ is not smooth due to the clipped denominator terms of y_j (see line 8 of Algorithm 2). We can easily fix this issue with a change of variables, defining $\langle \hat{v}_i, B\hat{v}_i \rangle$ in log-space. This results in Algorithm 3.

Specifically, define $[(v, Bv)]_j = e^{\log(\rho) + (\log(\nu) - \log(\rho))\text{sigmoid}(z_j)}$ where z_j is a newly introduced auxiliary variable. The relevant gradient with respect z_j is $\nabla_{z_j} = -(\langle v_j, Bv_j \rangle - [(v, Bv)]_j) \cdot [(v, Bv)]_j \cdot (\log \nu - \log \rho) \cdot \text{sigmoid}(z_j) \cdot (1 - \text{sigmoid}(z_j))$.

Regarding the still unresolved first issue, we could constraint $[B\hat{v}]_i$ to a ball with radius $\lambda_{\max}(B)$ centered at the origin, which is a convex set. Note that while a ball in \mathbb{R}^d is compact, it is not a Riemannian manifold anymore. A few works have developed theory for the setting that mixes convex and Riemannian optimization [24, 17]. Intuitively, we do not expect issues arising in our setting from the mixture of feasible sets, however, progress towards theoretic results takes time. We conjecture that Algorithm 3 is provably asymptotically convergent, although Algorithm 2 defined with clipping is a bit more practical.

Algorithm 3 Smooth Stochastic γ -EigenGame

```

1: Given: paired data streams  $X_t \in \mathbb{R}^{b \times d_x}$  and  $Y_t \in \mathbb{R}^{b \times d_y}$ , number of parallel machines  $M$  per player (minibatch size per machine  $b' = \frac{b}{M}$ ), step size sequence  $\eta_t$ , scalar  $\rho$  lower bounding  $\lambda_{min}(B)$ , scalar,  $\nu$  upper bounding  $\lambda_{max}(B)$ , and number of iterations  $T$ .
2:  $\hat{v}_i \sim \mathcal{S}^{d-1}$ , i.e.,  $\hat{v}_i \sim \mathcal{N}(\mathbf{0}_d, \mathbf{I}_d)$ ;  $\hat{v}_i \leftarrow \hat{v}_i / \|\hat{v}_i\|$  for all  $i$ 
3:  $[B\hat{v}]_i \in \mathbb{R}^d \leftarrow \hat{v}_i$  for all  $i$ 
4:  $z_i^0 \in \mathbb{R} \leftarrow 0$  for all  $i$ 
5: for  $t = 1 : T$  do
6:   parfor  $i = 1 : k$  do
7:     parfor  $m = 1 : M$  do
8:       Construct  $A_{tm}$  and  $B_{tm}$ 
9:        $[\langle v, Bv \rangle]_j = e^{\log(\rho) + (\log(\nu) - \log(\rho))\sigma(z_j)}$ 
10:       $\hat{y}_j = \frac{\hat{v}_j}{\sqrt{[\langle v, Bv \rangle]_j}}$ 
11:       $[B\hat{y}]_j = \frac{[B\hat{v}]_j}{\sqrt{[\langle v, Bv \rangle]_j}}$ 
12:       $\text{rewards} \leftarrow (\hat{v}_i^\top B_{tm} \hat{v}_i) A_{tm} \hat{v}_i - (\hat{v}_i^\top A_{tm} \hat{v}_i) B_{tm} \hat{v}_i$ 
13:       $\text{penalties} \leftarrow \sum_{j < i} (\hat{v}_i^\top A_{tm} \hat{y}_j) [\langle \hat{v}_i, B_{tm} \hat{v}_i \rangle [B\hat{y}]_j - \langle \hat{v}_i, [B\hat{y}]_j \rangle B_{tm} \hat{v}_i]$ 
14:       $\tilde{\nabla}_{im} \leftarrow \text{rewards} - \text{penalties}$ 
15:       $\nabla_{im}^{Bv} = (B_{tm} \hat{v}_i - [B\hat{v}]_i)$ 
16:       $\nabla_{im}^z = (\langle v_i, [Bv]_i \rangle - [\langle v, Bv \rangle]_i) \cdot [\langle v, Bv \rangle]_i \cdot (\log \nu - \log \rho) \cdot \sigma(z_i) \cdot (1 - \sigma(z_i))$ 
17:    end parfor
18:     $\tilde{\nabla}_i \leftarrow \frac{1}{M} \sum_m [\tilde{\nabla}_{im}]$ 
19:     $\hat{v}'_i \leftarrow \hat{v}_i + \eta_t \tilde{\nabla}_i$ 
20:     $\hat{v}_i \leftarrow \frac{\hat{v}'_i}{\|\hat{v}'_i\|}$ 
21:     $\nabla_i^{Bv} \leftarrow \frac{1}{M} \sum_m [\nabla_{im}^{Bv}]$ 
22:     $[B\hat{v}]_i \leftarrow [B\hat{v}]_i + \gamma_t \nabla_i^{Bv}$ 
23:     $\nabla_i^z \leftarrow \frac{1}{M} \sum_m [\nabla_{im}^z]$ 
24:     $z_i \leftarrow z_i + \gamma_t \nabla_i^z$ 
25:  end parfor
26: end for
27: return all  $\hat{v}_i$ 

```

F Alternative Parallelized Implementation

As mentioned in Section 5, we plan to open source our implementation, specifically the implementation used to conduct the neural CCA experiments described in Section 5.2.1. The specific parallelization we used was different than that implied by Algorithm 2. Instead, we parallelized the estimation of the matrix-vector products $A\hat{v}_i$ and $B\hat{v}_i$ for all i and then aggregated this information across machines. Figure 7 provides a diagram illustrating how data and algorithmic operations are distributed.

G Additional Experiments

In pursuit of understanding the regularization benefits of our stochastic approximation approach with a fixed step size, we explore various ways of regularizing the matrices A and B prior to calling `scipy.linalg.eigh(A, B)` to see if we can achieve a similar solution. Figure 8 explores various parameter settings, but none adequately recover the original signals.

We parameterize our regularizations as follows. Let $C = \mathbb{E}_t[x_t x_t^\top]$. Then

$$A = \mathbb{E}_t[\langle x_t, x_t \rangle x_t x_t^\top] - \text{tr}(C + \epsilon)(C + \epsilon) - 2(C + \epsilon)^2 \quad B = C + \epsilon'. \quad (88)$$

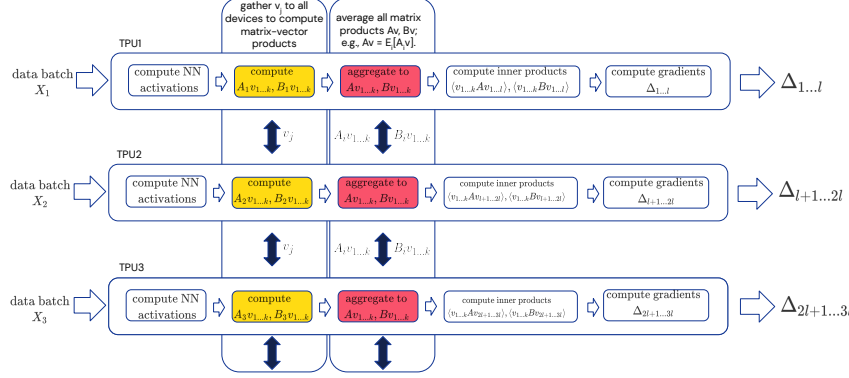


Figure 7: Parallelization of γ -EigenGame implementation for neural CCA experiments in Section 5.2.1.

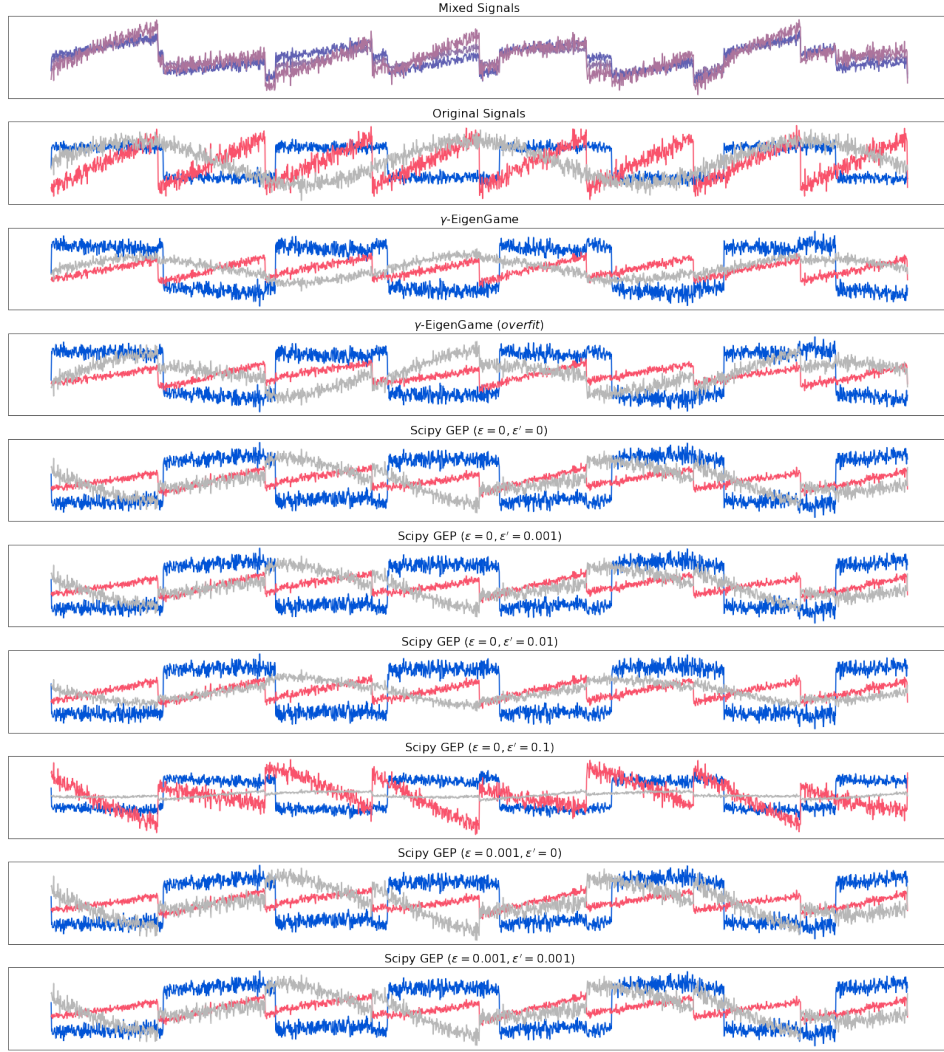


Figure 8: Figure 2 repeated with additional regularized versions of `scipy.linalg.eigh`.

H Hyperparameters and Experiment Details

H.1 ICA

Details of the unmixing experiment we run can be found on the scikit-learn website: [..../auto_examples/decomposition/plot_ica_blind_source_separation.html](http://scikit-learn.org/stable/auto_examples/decomposition/plot_ica_blind_source_separation.html) [33]. We solve for top-3 GEP formulation of ICA using $n = 2000$ samples taken from the time series data. Minimal hyperparameter tuning was performed. Learning rates were searched over orders of magnitude (e.g., 0.01, 0.1, 1.0, ...).

H.1.1 Comparison

The parameters used for Algorithm 2 (γ -EigenGame) in Figure 2 are listed in Table 1. Those for overfitting γ -EigenGame to the data are listed in Table 2.

Algorithm Parameters	
batch size b	$\frac{n}{4}$
M	1
# of iterations (T)	$10^3 \cdot \frac{n}{b}$
η_t	$10^{-2} \cdot \frac{b}{n}$
β_t	$1 \cdot \frac{b}{n}$

Table 1: Algorithm 2 hyperparameters for γ -EigenGame in Figure 2.

Algorithm Parameters	
batch size b	n
M	1
# of iterations (T)	10^5
η_t	10^{-3}
β_t	1

Table 2: Algorithm 2 hyperparameters for γ -EigenGame (*overfit*) in Figure 2.

H.1.2 Unbiased

Each of the plots in Figure 3 uses a different minibatch size b ; the hyperparameters used for Algorithm 2 are listed in Table 3 as a function of b .

Algorithm Parameters	
M	1
# of iterations (T)	$10^3 \cdot \frac{n}{b}$
η_t	$10^{-2} \cdot \frac{b}{n}$
β_t	$1 \cdot \frac{b}{n}$

Table 3: Algorithm 2 hyperparameters for Figure 3.

H.2 CCA

Details of both CCA experiments can be found below.

H.2.1 Comparison

Hyperparameters for the algorithm proposed in [30] are the same as in their paper. Their code is available on github at .../zihangm/riemannian-streaming-cca. We ran experiments 10 times to produce the means and standard deviation shading in Figure 2. We run PCA first on the data to remove the subspaces in X and Y with zero variance. We then solve the top-4 GEP formulation of CCA. Hyperparameters were tuned manually, searching over orders of magnitude (e.g., 0.01, 0.1, 1.0 and in some cases 0.05, 0.5, 5.0).

Shared parameters	
b	100
M	1
T	$\frac{n}{b}$
MNIST	
η_t	0.1
β_t	1.0
Mediamill	
η_t	50
β_t	5
CIFAR-10	
η_t	0.1
β_t	0.1

Table 4: Algorithm 2 hyperparameters for Figure 2.

H.2.2 Neural Network Analysis

We trained two CNNs for the $d > 10^3$ and $d > 10^5$ CCA (top-1024 GEP) experiments in Figure 5. Details of both architectures are listed in Table 5.

$$d = 2048 > 10^3 - \text{Figure 5 (left)}$$

Activations Harvested	Last convolutional layer and dense layer
Conv Layer Output Channels	[64, 32]
Conv Strides	[2, 1]
Dense Layer Sizes	[512]
Total Activations	$d_x = d_y = 58368$

$$d = 116736 > 10^5 - \text{Figure 5 (right)}$$

Activations Harvested	All convolutional layers and dense layer
Conv Layer Output Channels	[128, 256, 512]
Conv Strides	[1, 1, 1]
Dense Layer Sizes	[1024]
Total Activations	$d_x = d_y = 1024$

Table 5: CNN architecture parameters for CIFAR-10 Neural CCA experiment.

We used the hyperparameters listed in Table 6 for running γ -EigenGame.

Algorithm Parameters

b	2048 (256 per device)
M	8 (2×2 TPU = 4 chips, 2 devices/chip)
T	10^7
η_t	$t_c = 10^5$, $\eta_0 = 10^{-4}$, $\eta_T = 10^{-6}$
β_t	10^{-3}
ϵ	10^{-4}

Table 6: Algorithm 2 (with parallelism modifications from Section F) hyperparameters for Figure 5.

Adam($b1 = 0.9, b2 = 0.999, \epsilon = 10^{-8}$) was used for learning \hat{v}_i . We pair Adam with a learning rate schedule that consists of separate warmup and harmonic decay phases. We have a warmup period for the eigenvectors while the auxiliary variables and mean estimates are learned. During this period, the learning rate increases linearly until it reaches the base learning rate after the period ends (iteration t_c). This is followed by a decaying learning rate ($\propto \frac{1}{t + \Delta t}$) which reaches the final learning rate at iteration T .

For the purpose of generating the plots, we estimated Rayleigh quotients with a larger batch size than that used to estimate the eigenvectors themselves; specifically, we used 2048 for evaluation vs 256 for training.

Both experiments were 100% input bound, meaning the bottleneck in speed was computing neural network activations and passing them in minibatches to our algorithm. Therefore, our current runtimes are not indicative of the complexity of our proposed update rule. Alternatively, one could precompute all activations and save them to disk, however, this is memory intensive and we chose not to do this. For completeness, the $d > 10^3$ dimensional experiment ran at 4.7 ms per step on average, and the 10^5 experiment at 30.2 ms per step.

We do not have a breakdown of the runtime that separates CIFAR-10 data loading from neural network evaluation (computing activations) from EigenGame update from other processes. However, we can share that overall, the $d > 10^3$ dimensional experiment ran at 4.7 ms per step on average, and the 10^5 experiment at 30.2 ms per step.